NEW EXPERIMENTAL DATA AND WHAT IT TELLS US ABOUT THE SOURCES AND ACCELERATION OF COSMIC RAYS

W. R. WEBBER
Astronomy Department, NMSU, Las Cruces, NM, 88003, U.S.A.

(Received 28 January, 1997)

Abstract. This paper summarizes new data in several fields of astronomy that relate to the origin and acceleration of cosmic rays in our galaxy and similar nearby galaxies. Data from radio astronomy shows that supernova remnants, both in our galaxy and neighboring galaxies, appear to be the sources of most of the accelerated electrons observed in these galaxies. γ-ray measurements also reveal several strong sources associated with supernova remnants in our galaxy. These sources have γ-ray spectra that are suggestive of the acceleration of cosmic-ray nuclei. Cosmic-ray observations from the *Voyager* and *Ulysses* spacecraft suggest a source composition that is very similar to the solar composition but with distinctive differences in the ^{4}He, ^{12}C, ^{14}N and ^{22}Ne abundances that are the imprint of giant W-R star nucleosynthesis. Injection effects which depend on the first ionization potential (FIP) of the elements involved are also observed, in a manner similar to the fractionization observed between the solar photosphere and corona and also analogous to the preferential acceleration observed for high FIP elements at the heliospheric solar wind termination shock. Most of the ^{59}Ni produced in the nucleosynthesis of Fe peak nuclei just prior to a SN explosion appears to have decayed to ^{59}Co before the cosmic rays have been accelerated, suggesting that the ^{59}Ni is accelerated at least 10^{5} yr after it is produced. The decay of certain K capture isotopes produced during cosmic-ray propagation has also been observed for the first time. These measurements suggest that re-acceleration after an initial principal acceleration cannot be large. The high energy spectral indices of cosmic-ray nuclei show a significant charge dependent trend with the index of hydrogen being -2.76 and that of Fe -2.61. The escape length dependence of cosmic rays from our galaxy can now be measured up to $\sim$300 GeV nucl^{-1} using the Fe sec/Fe ratio. This escape length is $\sim P^{-0.50}$ above 10 GeV nucl^{-1} leading to a typical source spectral index of $(2.70\pm0.10)-0.50 = -2.20$ for nuclei. This is similar to the source index of -2.3 inferred for electrons within the errors of ±0.1 in the index for both components. Spacecraft measurements in the outer heliosphere suggest that the local cosmic-ray energy density is $\sim$2eV cm^{-3} – larger than previously assumed. Gamma-ray measurements of electron bremsstrahlung below 50 MeV from the Comptel experiment on CGRO show that fully 20–30% of this energy is in electrons, several times that previously assumed. New estimates of the amount of matter traversed by cosmic rays using measurements of the B/C ratio are also higher than earlier estimates – this value is now $\sim$10 g cm^{-2} at 1 GeV nucl^{-1}. Thus altogether cosmic rays are energetically a more important component of our galaxy than previously assumed. This has implications both for the types of sources that are capable of accelerating cosmic rays and also for the role that cosmic rays may play in ionizing the diffuse interstellar medium.

Table of Contents

Space Science Reviews **81:** 107–142, 1997.

1. Introduction

Since the discovery of cosmic radiation the question of the origin of these high energy particles has been an astrophysical problem of foremost importance. In this paper we shall examine new data on the elemental and isotopic composition of galactic cosmic rays as well as their energy spectra, including also information from radio and γ-ray emission within our galaxy and from nearby galaxies to take a fresh look at the question of cosmic-ray origin and acceleration.

The elemental and isotopic composition of cosmic rays and their energy spectra contain important clues for testing ideas and models about nucleosynthesis in stars and the evolution of shocks in the interstellar medium. Rapid progress toward a better understanding of these processes and problems has been made in recent years. This is a result of new measurements of the charge and isotopic composition of cosmic rays on the *Voyager* and *Ulysses* spacecraft, new cross section measurements which enable the interstellar propagational history to be unravelled and the imprint of the sources to be revealed, and measurements of the cosmic-ray spectra and composition at high energies, which provides an understanding of the acceleration process.

From simple energetic arguments, Ginzburg first demonstrated many years ago (Ginzburg and Syrovatskii, 1964) that supernova and their associated shocks are the most likely source of cosmic rays just because of the massive amount of energy and the extreme energies involved. Since that time the supernova models have been exploited and extended. But there are many questions yet to be understood. These include: (1) What is the origin of the material that is accelerated to cosmic-ray energies? Is it direct injecta from the supernova themselves, the hot component of the interstellar gas, or perhaps stellar wind particles in young OB associations where frequent supernova are occurring? (2) When and how does the acceleration occur? Is it early in the lifetime of the SNR (supernova remnant), or later when the expanding shocks have reached a scale size of several 10s of pc and shocks from other nearby SN may be overlapping? And after the initial acceleration is there further re-acceleration in the interstellar space – or even a more or less continuous acceleration of cosmic rays to high energies? (3) How much material have cosmic

rays traversed since their acceleration – and just what is the role of cosmic rays in galactic dynamics and does this in turn influence the acceleration process?

The new cosmic-ray measurements from various spacecraft that we wish to briefly summarize here and will describe more fully later with respect to their role in answering some of the questions posed above are as follows: (1) The decay of ^{59}Ni and the time of cosmic-ray acceleration. Starting with the ISEE-3 spacecraft (Leske, 1993) and including *Voyager* (Lukasiak et al., 1997b) and *Ulysses* (Connell and Simpson, 1997) measurements, all three of these spacecraft experiments have now confirmed the almost complete decay of ^{59}Ni into ^{59}Co. This electron capture isotope has a half-life of 7.5×10^4 year so the absence of any appreciable ^{59}Ni in cosmic rays means that the nucleosynthesis must have occurred $>10^5$ yr prior to the time the particles were accelerated. (2) It is now confirmed by *Voyager* measurements (Lukasiak et al., 1997a; Soutoul et al., 1997) that several K capture isotopes such as ^{49}V, ^{51}Cr and possibly ^{55}Fe, which are produced as secondaries during cosmic-ray propagation in the galaxy, have partially decayed – in particular $\sim$25% of the ^{51}Cr and ^{49}V isotopes have decayed. Since this decay is strongly energy dependent it may be used to infer whether there is any re-acceleration of cosmic rays after their initial acceleration (which is assumed to occur over a short time). These K-capture measurements indicate that there is possibly some re-acceleration but it is relatively small, perhaps 20% at most of the total final energy. (3) The nuclear composition of the cosmic-ray source as determined particularly by *Voyager* and *Ulysses* measurements is remarkably similar to the solar composition with only four isotopes, ^{4}He, ^{13}C, (or ^{12}C), ^{14}N, and ^{22}Ne out of $\sim$25 measured, showing any significant differences greater than $\sim$20% from that of solar composition (e.g., Lukasiak et al., 1997a). These compositional differences may be a direct barometer of the cumulative nucleosynthesis in the cosmic-ray sources. The specific isotopic differences noted above are in contrast to the atomic characteristics of the cosmic-ray source abundances which seem to reflect a first ionization potential difference relative to the solar photospheric abundances, suggesting acceleration in a hot environment similar to that of the solar corona which itself also exhibits first ionization potential differences relative to the photosphere. (4) Significant differences in the spectra of hydrogen and heavier nuclei from He to iron up to energies of a few TeV nucl^{-1}. This comparison is made possible by new measurements of the primary species at low energies along with new measurements of the individual elements at high energies up to and beyond 1 TeV nucl^{-1} using the Spacelab and Sokol experiments (Müller et al., 1991; Ivanenko et al., 1993) and large balloon borne detectors (Asakamori et al., 1993; Ichimura et al., 1993). These observations, when corrected for propagational effects, suggest that the accelerated energy or rigidity spectra of all species – including electrons, which have greatly different loss mechanisms, have similar spectral indexes in the range from -2.2 to -2.4, extending with only very small changes over 4–5 magnitudes of energy. This has obvious implications for the acceleration mechanism and its spatial and time scale.

In addition to the above new measurements which reflect directly on the galactic cosmic rays themselves, we should take note of other new observations that provide an understanding of the acceleration process itself.

The first of these is the observation of a new acceleration process that is occurring at the termination shock between the solar wind and the interstellar medium (Fisk et al., 1974; Pesses et al., 1981; Jokipii, 1986) – estimated to be at a distance 80–100AU from the Sun. This acceleration produces the so called anomalous cosmic rays (nuclei from H to Ne and above) accelerated to energies 10–100 MeV/nuc. These nuclei show a first ionization potential selection and appear to have a spectral index of -2.3–2.5 near the shock, very similar to the index for galactic cosmic rays. This nearby example of astrophysical shock acceleration shows that this process is probably commonplace in the vicinity of similar stars in the galaxy. It provides an example, which is subject to direct observation, of how the acceleration process may proceed in the much larger scale regions where the galactic cosmic rays are accelerated.

And finally radio astronomy measurements of the synchrotron spectra from SNR in our galaxy and in other nearby galaxies strongly support the suggestions that galactic cosmic-ray electrons are accelerated in the vicinity of these objects (Duric, 1994; Anderson and Rudnick, 1996). For the first time this association with SNR can now be extended to cosmic ray nuclei as well. The sensitivity of the EGRET experiment on GRO is such that it can now detect γ-rays from several nearby SNR individually with spectra that are characteristic of bremsstrahlung emission and nuclear interactions of nuclei accelerated with a spectral index of -2.1 to -2.3 near these objects (Esposito et al., 1996).

2. The Energetics of Cosmic Rays and Limits on the Types of Cosmic-Ray Sources

One of the most important properties of cosmic rays in terms of understanding their origin is simply the large amount of energy that they contain relative to other global processes in the galaxy. This energy content for our galaxy may be estimated a number of ways. It is important to recognize that new estimates of the local cosmic-ray energy density outside the heliosphere, based on the *Voyager* and Pioneer spacecraft interplanetary gradients, are higher than previous estimates. This energy density, ϵ, is now believed to be 2 eV cm^{-3} or about 3×10^{-12} erg cm^{-3} (Webber, 1987, 1994). In addition the amount of matter traversed by cosmic rays is estimated to be $\sim$10 g cm^{-2} at 1 GeV nucl^{-1} or about twice the typical earlier estimates (Webber, 1993). Both of these factors mean that cosmic rays play an even more important role in the dynamics of the interstellar medium, with an energy density at least as large as an average interstellar B field $\sim$5 μG. Diffusion models for cosmic ray propagation in the galaxy suggest that this energy density is maintained on average over a region $\sim$12 Kpc in radius with a half thickness

$\sim$1 Kpc corresponding to a volume $\sim 2.5 \times 10^{67}$ cm^3. Since the lifetime, τ, of the cosmic rays at $\sim$1 GeV nucl^{-1} is $\sim$20 Myr (Lukasiak et al., 1994), the total power requirement $P = \varepsilon V/\tau = 1.3 \times 10^{41}$ erg s^{-1}. This is a factor of roughly 3 higher than an earlier estimate by Axford, (1981), for example. A calculation using the amount of matter traversed by the cosmic rays leads to a similar power requirement (e.g., Drury, 1983).

This large power requirement constrains the kinds of sources that can account for the bulk of the cosmic rays in the galaxy. Even global processes such as spiral density waves seem to fall short, providing a net energy flow $\sim 6 \times 10^{40}$ erg s^{-1} (Duric, 1988). Only supernova and SNR seem to be able to provide enough power to account for galactic cosmic rays. The total amount of kinetic energy associated with a young SNR is $\sim 10^{51}$ ergs. Assuming that the frequency of type I or type II supernova is $\sim$1 every 50 years gives a total power of 7×10^{41} erg s^{-1}, barely enough, and requiring that the efficiency for particle acceleration be high, 10% or more (see also Drury, 1983). (See, however, the estimate by Dahlem et al., 1995, which gives a higher power estimate of $\sim 1.5 \times 10^{42}$ erg s^{-1}.) Any secondary acceleration mechanism/or re-acceleration for example, if it constitutes a significant fraction of the initial acceleration, must itself provide globally a few $\times 10^{40}$ ergs s^{-1} of energy input, a large value which needs to be considered when evaluating the efficiency of possible re-acceleration processes.

3. Astrophysical Evidence for Energetic Particle Acceleration

3.1. Evidence from radio astronomy

Astrophysical evidence in the form of photons provides a unique probe for the sites of particle acceleration in our galaxy and other galaxies. The principal diagnostic for electron acceleration is synchrotron radiation – mainly in the radio part of the spectrum. The synchrotron emissivity (*S*) has a direct dependence on the cosmic-ray electron density (*N*) and a non-linear dependance on the magnetic field strength (*B*). The relationship is given by $S \sim N B^{1+\delta}$ where δ is the synchrotron spectral index which is related to the energy spectrum of the electrons $N(E) = K E^{\gamma}$ where $\gamma = 2\delta + 1$. The relationship between the peak radio emission frequency and the energy of the individual electrons is given by ν(MHz) $\approx 8 B^2(\mu\text{G}) E^2$ (GeV), thus for a best estimate of the total galactic magnetic field of 6μG, (including both ordered ($\sim$2.5 μG) and disordered ($\sim$4.5 μG) components), e.g., see reviews by Beck et al. (1994); Zweibel and Heiles (1997) a range of frequencies between 10 MHz and 10 GHz corresponds to electron energies from $\sim$300 MeV to $\sim$10 GeV.

It is now possible to study the spectral index and total emissivity of $\sim$100 SNR in our galaxy and a large number in other nearby galaxies as well. In our galaxy the distribution of spectral indices for these SNR compiled from data given by Green (1984) and Berkhuijsen (1986) is shown in Figure 1. The average radio index is

-0.55 corresponding to an electron energy spectral index of -2.1. Selection effects may influence some of these spectra since it is unlikely that a simple spectral index is ever less than 0.5 as is observed. For our galaxy the total global radio spectrum actually measured (in the polar direction) is shown in Figure 2 (updated from Webber et al., 1980). This spectrum has an index -0.67 at frequencies between $\sim$30–600 MHz, steepening to -1.0 at frequencies $>$1GHz, somewhat steeper than the cumulative SNR spectra shown in Figure 1. The steepening with frequency is observed in many other nearby galaxies as well and follows directly from the diffusion and energy loss of the electrons as they move away from their sources into the disk and halo of the galaxy. The synchrotron loss rate for electrons is $dE/dt \sim B^2E^2$ erg s^{-1} so that a particle loses half of its energy in a characteristic time $\tau = E/dE/dt \sim B^{-2}E$ yr. This increasing loss rate with energy explains the general steepening of the galactic spectrum relative to the average SNR spectrum as the electrons populate the galaxy as a whole. This diffusion means that the intrinsic source spectrum is steepened and the distribution of the electrons is smeared on spatial scales $\sim d_S$ where d_S represents a diffusion scale length for electrons = 5 $(\nu/\text{GHz})^{-1/8}(B^2/\text{eV cm}^{-3})^{-1/2}$ Kpc. The synchrotron radio maps of our galaxy and others are thus blurred versions of the cosmic ray source distribution on a scale of a few Kpc.

It is possible to relate the source distribution of electrons inferred from radio measurements to specific types of sources within galaxies through the well established IR-radio correlation. This correlation, first discovered in the mid 1980s when the improved IR observations from IRAS spacecraft became available (e.g., Dickey and Salpeter, 1984), relates the IR emission at $\sim$60–100μ to the radio emission from 150 MHz to $>$10 GHz. A striking almost 1:1 correlation between the total radio and IR emission was first observed for galaxies as a whole (de Jong et al., 1985). Later when higher resolution IR measurements became available this study was extended to the features of individual galaxies – including our own (Beck and Golla, 1988; Bicay and Helou, 1990; Heikkila and Webber, 1994). It is now recognized that the largest fraction of this IR emission comes from IS dust locally heated to $\sim$40–60 K by young O–B stars in nearby H II regions (Devereaux and Eales, 1989). Since these stars are the progenitors of SN we have the immediate connection between the sources of energetic electrons as identified by the IR emission and the electrons themselves as identified by the more spatially diffuse radio emission.

This propagation picture is quantatively described by increasingly more sophisticated and realistic diffusion models for the propagation of these electrons both in the disk and from the disk into the halos of galaxies (e.g., Strong and Youssefi, 1997). The striking similarity of the scale size of the radio halo of our galaxy in Kpc and other similar spirals is confirmed from a study of 10 nearby edge-on spirals in which the characteristic scale of radio emission in the Z direction, Z_0, is found to be 1.0 ± 0.3 Kpc (Webber et al., 1994).

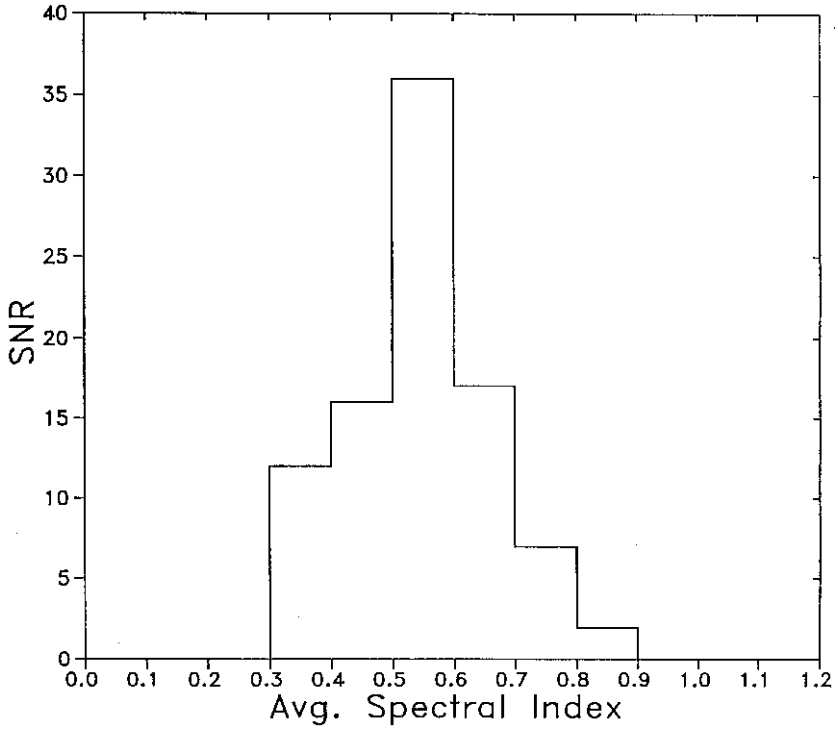

Figure 1. Distribution of the average spectral indices for radio synchrotron spectra of ∼100 SNR in our galaxy. (Compiled from data by Green, 1984; and Berkhuijsen, 1986.)

So the global picture of first the acceleration and then the diffusion of electrons from their sources out into the galaxy and into its halo for our galaxy and other nearby galaxies has advanced dramatically over the last few years. Quantitatively it is still not possible to make a correspondence between the total energy of the individual sources in our galaxy with the total synchrotron emissivity of our galaxy – mainly because all of the individual SNR cannot be observed. For other nearby galaxies it is also not possible to identify all of the SNR because the angular resolution is not good enough. However for M-33, a medium sized spiral only 2 Mpc away, Duric (1995) have made a careful study which has identified the radio emission from over 50 SNR. These 50 SNR have radio spectral indices distributed about a mean of -0.5 while the measured spectral index of disk emission from M-33 was found to be -0.9. This steepening could reasonably be described using a simple diffusion model with a diffusion coefficient depending on energy as $K(E) \sim E^{0.8}$, somewhat steeper than the $E^{0.6}$ dependence needed to describe the radio spectrum in our galaxy (Strong and Youssefi, 1997). The energetics of the individual SNR's were addressed using equipartition minimum-energy estimates. The total minimum energy of all of the currently active SNRs was found to be $\sim 7 \times 10^{51}$ ergs as compared with a total of 2×10^{54} ergs for the total radio emission from M-33.

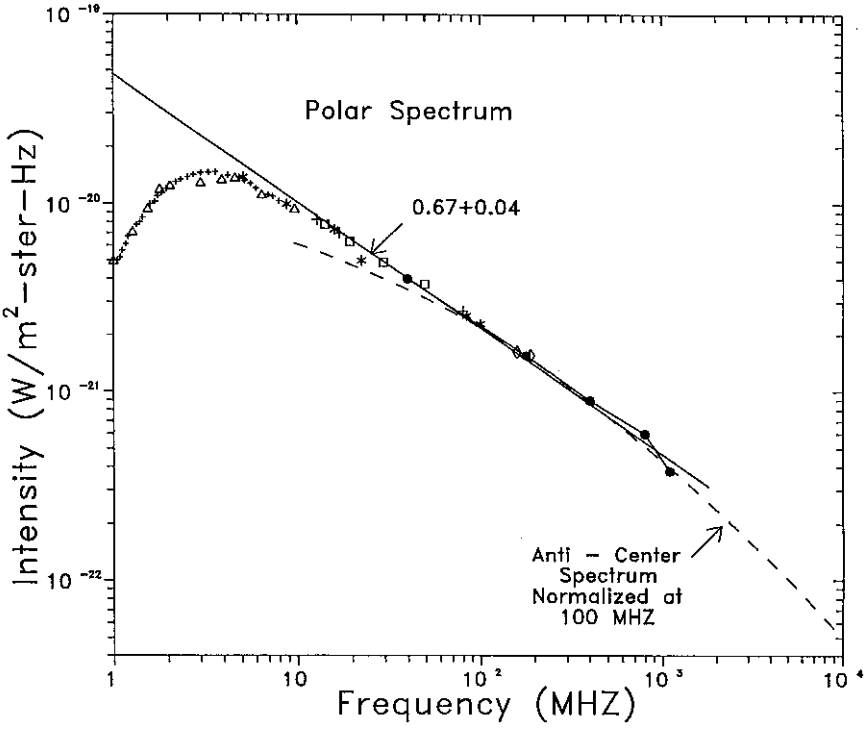

Figure 2. Total radio spectrum from our galaxy in the north polar direction. The radio spectral index of -0.67 is a fit to the data between 30 and 600 MHz. (Updated from Webber et al., 1980.)

This ratio of 300 for the energies could simply be the ratio of the leakage time of electrons from M-33 to the mean lifetime of a SNR. If SNR live $\sim 10^5$ yr, for example, this would imply a residence time for electrons in the disk of M-33 $\sim 3 \times 10^7$ yr, about what it is in our galaxy. Thus using plausible arguments, Duric et al. (1995) succeeded in showing that the SNR's in M-33 could reasonably account for the total distributed electron population in that galaxy.

Much progress has also been made in understanding where the acceleration might be occurring in SNR. Cas A is a particularly interesting object studied originally by Chevaliar and others (Chevaliar et al., 1976). Recently Anderson and Rudnick (1996) have reported a high-resolution VLA observation of Cas A including spectral index studies of localized regions, with the goal of understanding the physical nature of the particle acceleration. These studies identified many bright radio knots which could be localized regions of acceleration. These knots exhibited a large dispersion of spectral indices ranging from -0.5 to -0.9 whereas the average index of the remnant is -0.77. A picture in which the acceleration seems to be occurring in localized regions which have different characteristics on different time scales throughout the remnant seems to indicated by these studies.

So overall radio astronomy observations have played a crucial role in the understanding of where the electrons are accelerated and how they are redistributed throughout the galaxy, both in our galaxy and in nearby galaxies.

3.2. EVIDENCE FROM γ-RAY ASTRONOMY

Studies in γ-ray astronomy are playing an increasingly important role in determining the sites for the acceleration of cosmic-ray nuclei and for understanding the subsequent propagation of both the nuclei and electrons. This is important because γ-rays are the only astrophysical window providing information on the nuclei. These nuclei are believed to account for the bulk of the energy going into accelerated particles. For nuclei the main γ-ray emission mechanism is through nuclear interactions with the ambient material. This produces π° which decay immediately into two γ-rays with a characteristic 'rest energy' peak at $\sim$70MeV. The γ-ray spectrum from such interactions falls off rapidly at lower energies, has a peak at $\sim$100 MeV, and falls off at higher energies with a spectrum very similar to that of the cosmic-ray nuclei producing the interactions. The γ-ray emissivity, $S\gamma$, along a line of sight is proportional to the matter density, $n_{\rm H}$, $\times$ the cosmic-ray nuclei density $N(E)$, e.g., $S\gamma \sim \int n_{\rm H} N(E)\ {\rm d}r$. Another very important process of γ-ray emission is bremsstrahlung from energetic electrons passing near ambient interstellar nuclei. For this relativistic bremsstrahlung the γ-rays have an energy which is a large fraction of the initial energy of the electron. The emissivity from this process is also a product of $n_{\rm H}\times$ the cosmic-ray electron density $N_e(E)$. The spectrum of bremsstrahlung γ-rays maps out the spectrum of the producing electrons but since this spectrum extends to lower energies than that from π° decay, the bremsstrahlung emission may actually dominate the γ-ray spectrum below $\sim$50 MeV. This provides a window on the low energy electron spectrum not available from radio astronomy.

The first instrument to seriously map the γ-ray distribution in our own galaxy, Cos-B, was mainly sensitive to γ-rays $>$70 MeV and so was able to provide the first indication of the distribution of energetic nuclei in our galaxy through the π° decay spectrum. A plot of the radial distribution of nuclei as inferred from the γ-ray distribution measured by Cos-B is illustrated in Figure 3 (Bloemen et al., 1993). This figure also shows calculations for a diffusion model starting with a given source distribution. The radial dependence of nuclei also appears to be consistent with the radial distribution of cosmic-ray electrons as derived from radio maps (Webber et al., 1992). Both of these distributions show a much flatter radial fall off than the rather poorly known radial distribution of SNR. However, diffusion models have been able to show that the observed radial distribution of both nuclei and electrons in our galaxy are consistent with the diffusion of these particles away from their sources which are assumed to be SNR (Bloemen et al., 1993; Webber et al., 1992).

The γ-ray results from the CGRO have moved this study to a new level of precision and sensitivity. These results come from the EGRET experiment at energies

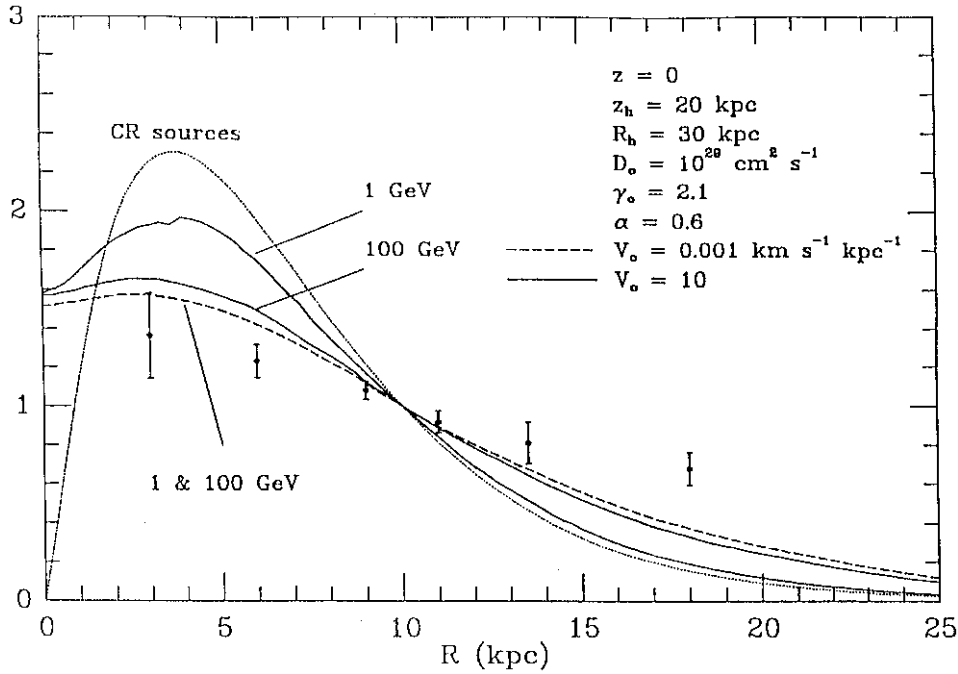

Figure 3. Radial distribution of nuclei in our galaxy as inferred from γ-ray measurements from Cos-B above 100 MeV (solid data points). (From Bloeman et al., 1993.) Also shown are predictions of a diffusion model starting from an assumed source distribution of SNR.

$>$30 MeV and the COMPTEL experiment at energies from 1–30 MeV. From these new measurements it has been possible to; (1) observe γ-rays from at least one external galaxy, the LMC (Sreekumar et al., 1992), (2) observe γ-rays from energetic nuclei interacting with ambient matter in SNR, the much sought after 'smoking gun' for the detection of accelerated nuclei, along with electrons, in these sources (Esposito et al., 1996), and (3) provide a potentially much better indication of the distribution of nuclei and electrons in our galaxy as well as a determination of the spectrum of γ-ray emission over a much wider energy range than from Cos-B and earlier experiments.

Expanding on point (3) above first we show in Figure 4 the γ-ray emissivity spectrum derived from both EGRET and COMPTEL data along with predictions from a diffusion model by Strong and Youssefi (1997) assuming a source spectral index $= -2.3$ for both electrons and nuclei. This figure shows that the γ-ray emissivity derived from the γ-ray data from both Cos-B (high energies) and COMPTEL (low energies) is consistent with predictions based on the directly measured spectra of the electron and nuclei components at the Earth. The relative contributions of the nuclei component (π° decay) and electrons (bremsstrahlung) to the total γ-ray emission are now clearly seen for the first time in this data. Also the flattening of the electron spectrum below $\sim$100 MeV caused by ionization losses is seen in both

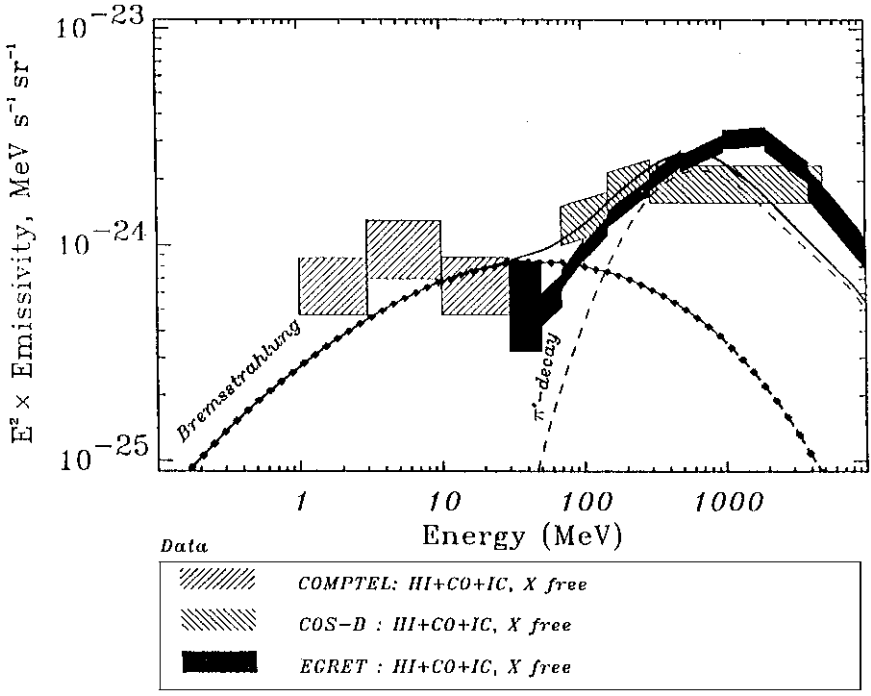

Figure 4. The γ-ray emissivity spectrum from our galaxy as deduced from EGRET and COMPTEL measurements on GRO. Predictions from a diffusion model are also shown as solid lines. (Strong and Youssefi, 1997.)

the COMPTEL data and the predictions. The EGRET emissivities above $\sim$1 GeV are almost a factor of two higher than the predictions based on the nuclei spectrum at the Earth (Hunter et al., 1997). At the present time it is not clear whether this is due to an underestimate of the local IS nuclei flux above $\sim$10 GeV or the fact that the γ-ray emissitivity is derived from the γ-ray spectrum from the galactic center which may represent a different nuclei flux than that found locally (Mori, 1997).

Deriving the radial variation of cosmic-ray nuclei and electrons in the galaxy from the γ-ray data is also complicated. The radial distribution derived for $\sim$2 GeV nuclei and 1 GeV electrons by Strong and Youssefi (1997) using the γ-ray emissivity from the EGRET analysis above $\sim$100 MeV (Strong and Mattox, 1996) is shown in Figure 5. These profiles are similar to earlier profiles obtained using Cos-B data (Bloemen et al., 1993) but seem to show more structure, possibly related to spiral arms. These profiles are generally much flatter than possible SNR profiles. This is understandable because of the characteristic smearing of 1–2 Kpc resulting from cosmic-ray diffusion. Overall this new data continues to make a strong case for the origin of both cosmic-ray nuclei and electrons in or near SNR. The relative abundance of nuclei and electrons (with the electron energy spectra now extending to much lower energies) clearly shows that earlier estimates that the electrons

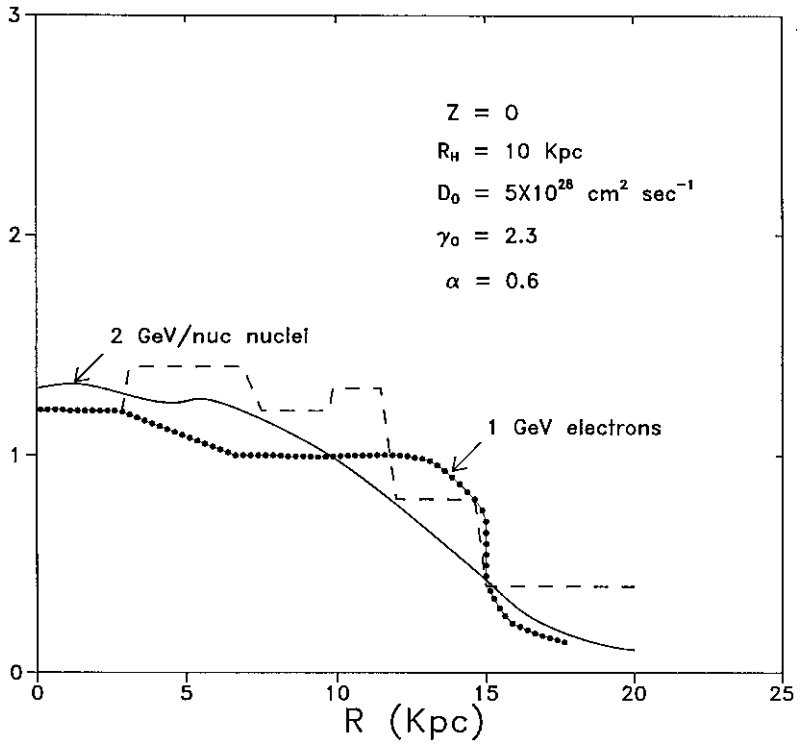

Figure 5. Radial distribution of 2 GeV nucl^{-1} nuclei and 1 GeV electrons (shown as solid lines) as compared with the >100 MeV emissivity derived from the analysis of EGRET data (shown as a dashed line). (Adapted from Strong and Youssefi, 1997.)

contain only a few percent of the energy of the accelerated particles greatly underestimate their contribution. On an energy basis a better value as obtained from the low energy γ-ray data would be ~20–30%, and in terms of total number density the two species are roughly equal. This relative energy density for electrons is consistent with the estimates of Dahlem et al. (1995) who find for our galaxy, from radio considerations, that $\epsilon_{\text{elect}} \sim 0.6$ eV cm^{-3} or about 30% of the total CR energy estimate of 2 eV cm^{-3} noted earlier.

With regard to points (1) and (2) above we observe the following. The LMC has now been weakly detected in γ-rays >100 MeV by EGRET (Sreekumar et al., 1992). The observed intensity of these γ-rays is consistent with the radio emission from this galaxy assuming the same ratio of nuclei to electrons as in our own galaxy. This source is too weak to provide a measurement of the γ-ray spectrum so it must be assumed that the >100 MeV γ-rays are indeed from the π° decay signature of nuclear interactions. It is nevertheless an important step and points the way toward future detection and even mapping of other nearby galaxies such as M-31 and M-33.

Relevant to the acceleration of cosmic-ray nuclei in our own galaxy is the observation by Esposito et al. (1996) using EGRET data, of γ-rays from several SNR in our own galaxy. This γ-ray emission may be the first detection of a signal from cosmic-ray nuclei accelerated in the shocks of the SNR, in much the same way that radio measurements have pointed to the acceleration of electrons in SNR both in our galaxy and M-33. At the present time the information on the γ-ray spectra of these SNR is very limited, however, so it is not possible to separate clearly the bremsstrahlung component due to electrons from the nuclei component. As a result one needs to be cautious in the interpretation of these measurements. Work is still in progress to improve the sensitivity of the data and to correlate the radio and γ-ray emission from specific SNR. This may help strengthen the case for one of the most significant measurements so far in the quest to determine the sources of cosmic-ray nuclei.

4. Theoretical Models for the Acceleration and/or Re-acceleration of Cosmic Rays

The main emphasis in this review is on experimental measurements related to the sources and acceleration of cosmic rays. For this reason we only summarize here the features of the cosmic-ray acceleration models that may be most relevant to the observations themselves. Excellent reviews of the physics of cosmic-ray acceleration may be found in papers by, e.g., Axford (1981), Drury (1983), Volk (1984), Blandford and Eichler (1987), and Jones and Ellison (1991). We will, however, discuss in more detail the process of re-acceleration or post acceleration. We will also discuss the newly observed particle acceleration occurring near the solar wind termination shock.

4.1. Shock acceleration models in SNR

The reviews of the cosmic-ray acceleration process generally focus on one form or another of shock acceleration. This emphasis probably has its origin in the seminal paper of Chevaliar et al. (1976), who directly related features of the radio emission of the SNR Cas A, to the acceleration of energetic electrons by the second order Fermi mechanism. Many authors followed this lead but attention soon turned to first-order Fermi acceleration near the high velocity shocks in SNR which carried much of the energy. One of the most useful of these new calculations was the work of Blandford and Ostriker (1978, 1980). This work not only demonstrated the characteristic $2 + \epsilon$ spectral exponent of the high energy particles, where $\epsilon \sim 0.2$ or 0.3 for strong shocks, but also presented a low energy spectrum that essentially turned over and was a remarkably good fit to the low energy interstellar spectrum deduced from measurements made near the Earth (Ip and Axford, 1985; Webber, 1987). This low energy spectrum was largely dominated by the effects of re-acceleration – further acceleration of the cosmic rays by weaker shocks as

the SNR expanded to ∼100 pc. This concept of a significant time period for the primary acceleration of cosmic rays was a valuable ingredient in the overall picture. In their picture the injection process was treated in an *ad-hoc* fashion; however, it now seems clear that the charge composition and ionization state of the material in the SNR must be an important part of this injection process leading to the observed composition of the cosmic rays.

The interaction of the cosmic rays with these shocks has been explored in ever increasing detail – including Monte Carlo models which consider the not inconsiderable pressure of the accelerated ions themselves (Ellison and Reynolds, 1991). The radio spectra of SNR can now be quite accurately reproduced (Reynolds and Ellison, 1992). It seems quite plausible that ∼10–20% of the initial energy of the SN explosion can eventually find its way into accelerated particles (e.g., Drury, 1983) – a number which is necessary for the energetics of the acceleration process as discussed earlier.

Recent activities in shock acceleration have focused more on the injection process itself in an attempt to reproduce the observed cosmic-ray charge composition, and on the energy spectra of the individual charges themselves including the maximum energy of the acceleration process (e.g., Biermann, 1996). A picture in which the SNR cosmic rays represent an accelerated mixture of interstellar or circumstellar gas and dust (Meyer et al., 1997; Ellison et al., 1997) is particularly interesting. This is the most serious attempt we are aware of to evaluate the entire process of injection and acceleration with the goal of explaining the specific abundance anomalies that have been observed in the cosmic-ray source as well as taking into account the acceleration in a non-linear way. The most prominent of the abundance anomalies, relative to solar composition, are according to these authors; (1) the low H, He and N abundances (the *Q/A* or FIP effect) and (2) the large enhancements of ^{22}Ne, ^{12}C and ^{16}O. In their picture the ^{22}Ne, ^{12}C and ^{16}O enhancements come from the most massive SN which accelerate their own ^{22}Ne–^{12}C–^{16}O enriched pre-SN Wolf–Rayet (W–R) wind material found locally within the acceleration volume.

A re-analysis of the observed cosmic-ray chemical composition in their paper leads to the conclusion that the cosmic-ray source material consists mainly of two components (in addition to the W–R component noted above) both originating in the interstellar or circumstellar medium; volatile elements from a gas phase and refractory elements from dust grains. This picture replaces the well known FIP effect and arises because, in addition to the depletion of the high FIP elements, the abundances of the elements Na, P, Ge, and Pb are found to be non-solar as well. This model makes specific predictions for the spectra of various nuclei – leading to slight differences in the spectra for individual charges as well as a slight flattening of the spectra above $\sim 10^{12}$ eV nucl^{-1} – but below the maximum accelerated energy $\sim 10^{14}$ eV nucl^{-1}. These predictions are illustrated in Figure 6, taken from their paper. We will take a closer look at these predictions and the composition and spectral measurements in a later section.

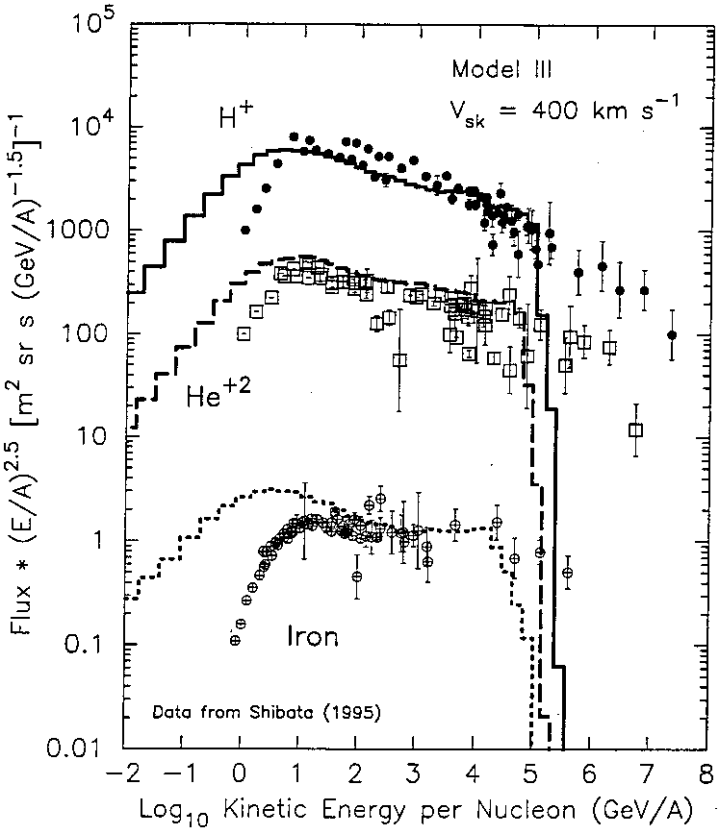

Figure 6. Comparison of measurements of the high energy spectra of H, He, and Fe nuclei and predictions. (From Ellison et al., 1997.)

4.2. ACCELERATION AT THE SOLAR WIND TERMINATION SHOCK

The previous discussion points up the value of having a nearby astrophysical accelerator of cosmic rays in the form of the solar wind termination shock. The story behind the discovery of this source has its origin in 1973 with the observation of turn-ups in the spectra of N and O nuclei at low energies at the Earth (Hovestadt et al., 1973; McDonald et al., 1974). Because these turn-ups were unexpected, these particles were called anomalous cosmic rays. Noting that both of these charges had a high FIP, Fisk, Kozlovsky and Ramaty (1974) made a suggestion as to their origin which has come to be commonly accepted – namely that these particles originate as interstellar neutrals (neutral because of their high FIP) which enter the heliosphere, are then ionized and swept out by the solar wind and finally accelerated in the outer heliosphere. The exact acceleration mechanism was not specified in this early model. Since this earlier work several other species, H, He, Ne, and Ar,

all high FIP elements, have been found to be enhanced at low energies thus lending further substance to the original suggestion by Fisk et al. (1974).

It soon became clear that the most likely source for the acceleration of these particles was at a solar wind termination shock now believed to exist at a distance where the outward solar wind pressure is balanced by the interstellar magnetic field and plasma pressure. Theories for the acceleration of these particles at this shock were developed (e.g., Pesses et al., 1981; Jokipii, 1986, 1990). In the theory by Jokipii drift along the shock is an important component of the acceleration. This drift, the direction of which depends on the alternating 11 year solar magnetic field polarity change, can accelerate protons up to $\sim$250 MeV and heavier ions up to a maximum energy $\sim(1/A) \times 250$ MeV nucl^{-1}, as is observed.

This termination shock acceleration is a directly observable process that does accelerate cosmic rays and the injection process is related to the FIP of the elements involved. Other nearby examples of shock-drift acceleration may also be found at the Earths bow shock and possibly interplanetary shocks as well (e.g., Decker, 1988). Stellar wind spectra suggest that FIP effects could be prevalent in these sources as well.

Recent measurements have estimated that the solar wind termination shock location is at $\sim$85 AU and have also determined that the accelerated spectrum is $\sim P^{-2.5}$, thus suggesting that this is a fairly weak shock with a Mach number $M = 2.4$ (Stone et al., 1996). These authors estimate that $\sim$5–10% of the solar wind energy may eventually go into the acceleration of these anomalous cosmic rays. It is interesting to speculate that such shocks, both much stronger and weaker, probably exist around $\sim 10^9$ other stars in the galaxy. Considering in the case of the Sun, a solar wind energy flow $\sim 3 \times 10^{27}$ ergs s^{-1}, converted with an efficiency $\sim$10%, implies a total galactic energy input $\sim 3 \times 10^{36}$ ergs s^{-1} from these sources, not quite comparable with that supplied by SNR, but certainly worth thinking about in terms of an injector of cosmic rays or a supply of low energy ions for the interstellar medium.

4.3. RE-ACCELERATION OF COSMIC RAYS

The concept of re-acceleration or continuous acceleration of cosmic rays during their propagation through the galaxy has its origin dating back to the ideas of Fermi (1949). In his picture cosmic-ray acceleration occurred gradually by repeated interactions with magnetic fields which produced both first- and second-order Fermi acceleration. These early ideas were largely supplanted by the shock acceleration theories that were developed in the late 1970s as well as by the realization that no adequate energy source for global cosmic-ray acceleration existed outside of SNR. The estimates of the available energy in interstellar turbulence or even in organized motions connected with the galactic spiral structure seemed to fall 1 or 2 orders of magnitude short of that available in SNR (Duric, 1988).

Letaw et al. (1984) looked at this problem of reacceleration again and proposed that the acceleration of cosmic rays is distributed over their propagation during which time the cosmic rays gain a factor of about 5 in energy. This conclusion was based on a comparison of the measured and predicted abundances of several secondary charges and isotopes at low energy. Improved cross section measurements and improved data have now greatly reduced the discrepancies pointed out by Letaw et al., however these authors also pointed out in this paper (along with Raisbeck et al., 1975) the importance of certain K capture isotopes for understanding the cosmic-ray propagation and possible re-acceleration. Several isotopes such as ^{49}V, ^{51}Cr, and ^{55}Fe, which are produced entirely as secondaries during the cosmic-ray propagation, have a probability as high as 50% at $\sim$200 MeV nucl^{-1} for electron attachment during propagation with subsequent decay by electron capture. This attachment probability is strongly energy dependent and can serve as a probe for the energy at which the attachment occurs and so provide a measure of possible re-acceleration effects.

Later Simon et al. (1986) carried this picture a step further by calculating the effect of re-acceleration on the cosmic-ray B/C ratio. They found that the observed ratio and its dependence on rigidity could be explained by a much flatter escape length $\sim R^{-0.33}$ if re-acceleration occurred instead of the dependence $\sim R^{-0.6}$ needed if no re-acceleration occurred. The amount of re-acceleration necessary to do this amounted to a factor $\sim$2. An escape length $\sim R^{-0.33}$ implies that the interstellar diffusion is dominated by a Kolmogorov type of turbulence spectrum which also has a $R^{-0.33}$ dependence. Such a weak rigidity dependence for the escape length fits in better with the small anisotropies observed above 10^{12} eV, and also with measurements of the spectra of the cosmic-ray nuclei themselves which suggest an exponent ~ -2.70 at high energies. The argument here follows from the assumption that the observed high-energy spectral index ($\sim$2.70) minus the escape dependence ($\sim$0.33) equals the source spectrum (2.37) with the -2.37 index being more understandable than an index of -2.10 or -2.20, for example. A factor of 2 re-acceleration needed in this picture would have a profound effect on the spectra of primary nuclei, however, particularly at low energies. Several papers appeared soon afterward examining re-acceleration effects for electrons, protons, helium nuclei and heavier species. This activity reached a peak in 1987, and is well summarized in a review paper by Cesarsky (1987). Among the things pointed out by Cesarsky were the following:

(1) In order for the re-acceleration to significantly modify the B/C ratio at energies between 1–10 GeV nucl^{-1}, as is required by the data, the magnitude of the re-acceleration must be roughly the same as the initial acceleration itself – a lot of energy must be available to provide this re-acceleration.

(2) When re-acceleration is introduced the escape length dependence flattens at high energies (to the exponent of the rigidity dependence of the turbulence spectrum causing the re-acceleration).

(3) Re-acceleration effects do not solve the low energy charge ratio problems (e.g., the ^{15}N/O ratio) for which they were originally proposed.
(4) Re-acceleration also causes a considerable modification of the low energy part of the spectra of primary nuclei such as H, He, C, O, and Fe.

Basically re-acceleration models are now introduced to explain two perceived problems associated with conventional galactic propagation models. These problems are related. First, it is observed that between ∼1–10 GeV nucl^{-1} the rigidity dependence of both the B/C and Fe sec/Fe ratios is proportional to $R^{-0.6}$ as noted earlier. This exponent is assumed to give directly the amount of matter traversed as a function of rigidity and so is a measure of the rigidity dependence of the (diffusion) escape of cosmic rays from the galaxy. If this steep dependence extends to very high energies ($>10^{12}$ eV) then the escape length becomes small very quickly leading to possible conflicts with cosmic-ray anisotropy measurements. This high value for the index of the escape length dependence also leads to a problem which is related to the cosmic-ray spectral index itself as noted earlier. At high energies, $\sim 10^{11}$ eV and above, the spectral index of most cosmic-ray primary components, H, He, O, and Fe appears to be about -2.70 (see later section which discusses this spectral index and how well it is known). For a particular escape length dependence δ, the measured cosmic-ray index at high rigidities, γ, is related to the source spectral index S by $\gamma = S + \delta$. Therefore a measured value of $\gamma = -2.70$, for example, translates into a source index, $S = -2.10$, if the escape dependence is assumed to be $\sim R^{-0.6}$. The source index required to explain features of the low energy spectra of nuclei is usually found to be closer to -2.3, however. If substantial re-acceleration occurs and the escape length dependence at high energies is smaller (e.g., $\sim R^{-0.33}$) a source spectral index closer to -2.3 can be obtained. It should be noted, however, that Biermann (1996) has discussed a situation in which the energy dependence of the escape time and the grammage traversed could well be different. In this case a simple addition of spectral indices as discussed above may not be appropriate.

In recent years, several new attempts have been made to evaluate the effects of re-acceleration (Letaw et al., 1993; Seo and Ptuskin, 1994; Heinbach and Simon, 1995). It is not easy to compare the predictions of these different models, however, because different re-acceleration coefficients are used in each paper. Using the model of Heinbach and Simon (1995) as an example, we note that the re-acceleration is described as before by a rigidity dependence $\sim R^{-0.33}$ which is essentially a Kolomogorov spectrum of irregularities. The acceleration coefficients are chosen so as to reproduce the observed B/C dependence which is $\sim R^{-0.6}$ between ∼1–10 GeV nucl^{-1}. This re-acceleration, in effect, pushes up the low-energy part of the secondary spectrum more than the higher-energy part and more than the primary spectrum thus producing the observed B/C dependence $\sim R^{-0.6}$ even though the underlying dependence on diffusion is $\sim R^{-0.33}$. To do this requires that the total amount of re-acceleration at ∼1 GeV nucl^{-1} be ≥50% of the particles initial energy. At higher energies, as re-acceleration becomes less effective, the B/C (and

Fe sec/Fe) ratio dependence should approach the underlying dependence chosen for the diffusion (re-acceleration) which is $\sim R^{-0.33}$ and is flatter than that observed between 1 and 10 GeV nucl^{-1}. This appears to be the prediction in both the Heinbach and Simon (1995) and also the Seo and Ptuskin (1994) papers. We will show later that new data on the Fe sec/Fe ratio up to several hundred GeV nucl^{-1}, while it shows some flattening of the dependence above 10 GeV nucl^{-1}, does not seem to approach a $P^{-0.33}$ spectral dependence at high energies. Both of the above papers do not unfortunately address the spectral effects on the primary nuclei at lower energies in sufficient detail; however Webber et al. (1992) using *Voyager* data on several primary nuclei at low energies and low modulation levels, conclude that the expected re-acceleration effects are not present in this data.

Overall the present re-acceleration models seem to us to create at least as many problems as they solve. It is true that, given enough re-acceleration, the $R^{-0.6}$ dependencies of the B/C and Fe sec/Fe ratios between 1–10 GeV nucl^{-1} can be explained using a less strong rigidity dependence of the diffusion. As a result the source spectral index that is needed to explain the observed high energy index of -2.70 becomes larger, e.g., -2.3–2.4, however, other expected re-acceleration effects are not always seen. Also there are other explanations for some of these effects of re-acceleration (see later section). What is strongly needed is more positive evidence of re-acceleration or lack of it. This evidence may soon be forthcoming using K capture nuclei measurements as described in a later section of this review.

5. New Cosmic-Ray Observations and their Relation to the Sources and Acceleration

In the following section we shall summarize some new cosmic-ray measurements that provide insights into the cosmic-ray sources and the acceleration process.

5.1. The charge composition measurements – the FIP effect

A considerable refinement of the deduced source composition of cosmic rays has occurred in the last few years. This has been made possible by improvements in both cross sections which enable the propagation to be modelled more accurately, and improvements in the measurements, particularly at low energies from the *Voyager* and *Ulysses* spacecraft to go along with the updated higher energy measurements from the HEAO spacecraft originally made in 1978–1980 (Engelmann et al., 1990). In Table I we show in column 1 the average cosmic-ray source composition deduced by *Voyager* experimenters (Lukasiak et al., 1997a) and *Ulysses* experimenters (Duvernois and Thayer, 1996) both of which use the updated HEAO data at higher energies in their analysis.

Significant improvements have also occurred in our understanding of solar coronal abundances as deduced from solar cosmic-ray measurements. These abund-

Table I
Relative abundance of charges in various astrophysical populations

Charge	CRS		LG∼Photosphere		SC	
2	10 700	± 10%	272 000 G&A 180 000 C		37 500	
6	443	± 16	1 010		286	± 20
7	24.1	± 3	313		78	± 3
8	536	± 10	2 380		632	± 20
10	63.6	± 4	340	± 48	93	± 7
11	3.9	± 0.4	5.7	± 0.4	7.0	± 0.7
12	105.5	± 2	107	± 4	123	± 5
13	8.3	± 0.4	8.5	± 0.3	9.5	± 0.8
14	100		100		100	
15	0.9	± 0.15	1.0	± 0.1	0.45	± 0.1
16	13.6	± 0.5	50.5	± 6.7	21.8	± 0.9
18	1.85	± 0.2	10.1	± 0.6	22	± 0.2
19	0.40 ss		0.4	± 0.03	0.33	± 0.07
20	6.1 ss		6.1	± 0.4	7.1	± 0.3
22	0.25 ss		0.25	± 0.01	0.30	± 0.10
24	1.5 ss		1.4	± 0.1	1.48	± 0.27
25	1.1 ss		1.0	± 0.1	0.54	± 0.18
26	100.5	± 3	90	± 2.4	96.5	± 6
27	0.23 ss		0.23	± 0.01	–	
28	5.1	± 0.3	5.0	± 0.3	4.0	± 0.5
30	0.085	± 0.010	0.125	± 0.01	0.075	± 0.025

ss = solar system percentages relative to Fe (consistent with CRS extrapolation).

ances are important for comparison with the cosmic-ray source abundances and also with the nominal solar system (or local galactic, LG) abundances as deduced mainly from meteoritic studies. The LG abundances from Grevesse and Anders (1989, G&A), are shown in the 2nd column of Table I. The solar coronal (SC) abundances shown in column 3 of Table 1 represent an average of those deduced from solar cosmic rays by Garrard and Stone (1993) and Reames (1995). These coronal composition estimates generally agree to within ±10%.

The data tabulated in Table I may be used in several ways to examine compositional differences between the cosmic-ray source (CRS) and solar system material. The most common way is to plot the ratios CRS/LG or SC/LG vs the FIP (first ionization potential) of the elements. This type of plot for both ratios is shown in Figure 7. The deficiency of high FIP elements in both the CRS and the SC is clearly seen. This effect for both types of sources was noticed as early as 1975 (Webber, 1975) and has been the input for believing that a FIP effect is operating in the cosmic-ray sources in a manner similar to that in the hot solar corona. The effect seems to set in at a FIP ∼9 eV and by 10–12 eV becomes saturated so

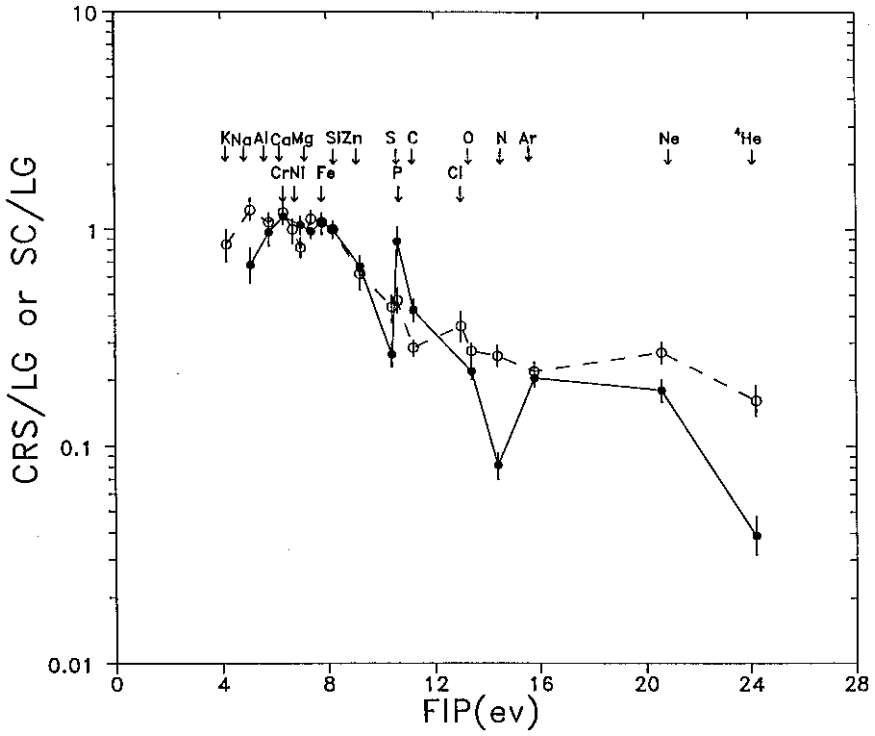

Figure 7. The ratios CRS/LG = solid circles, and SC/LG = open circles, as deduced from Table I, shown as a function of FIP.

that the abundances of the high FIP elements in both sources are on average only $\sim 0.2\times$ the abundances of the low FIP elements relative to the LG abundances (or abundances in the solar photosphere). There are significant differences on a charge by charge basis of the relative abundances in the CRS, however.

In an attempt to understand these differences better we show in Figure 8 a plot of the CRS/LG ratios vs the CRS/SC ratios – in effect a correlation of the two ratios where at least one of the sources (SC) apparently has a FIP effect operating. Here the ratios fall into 3 distinct classes lying along similar regression lines. We have the low FIP elements (line 1), the intermediate FIP elements (dotted line) and the high FIP elements (line 2). Along each line the different elemental abundance ratios are distributed in a way not related to FIP. This suggests that, if indeed FIP is partially responsible for organizing the abundances in *both* the SC and CRS, then some other effects are influencing the relative abundances in these two sources. These effects could be related to the source itself (e.g., nucleosynthesis) or to volatility effects.

There are many possibilities but before we speculate further on this charge compositional data let us now see what the isotopic composition data tells us.

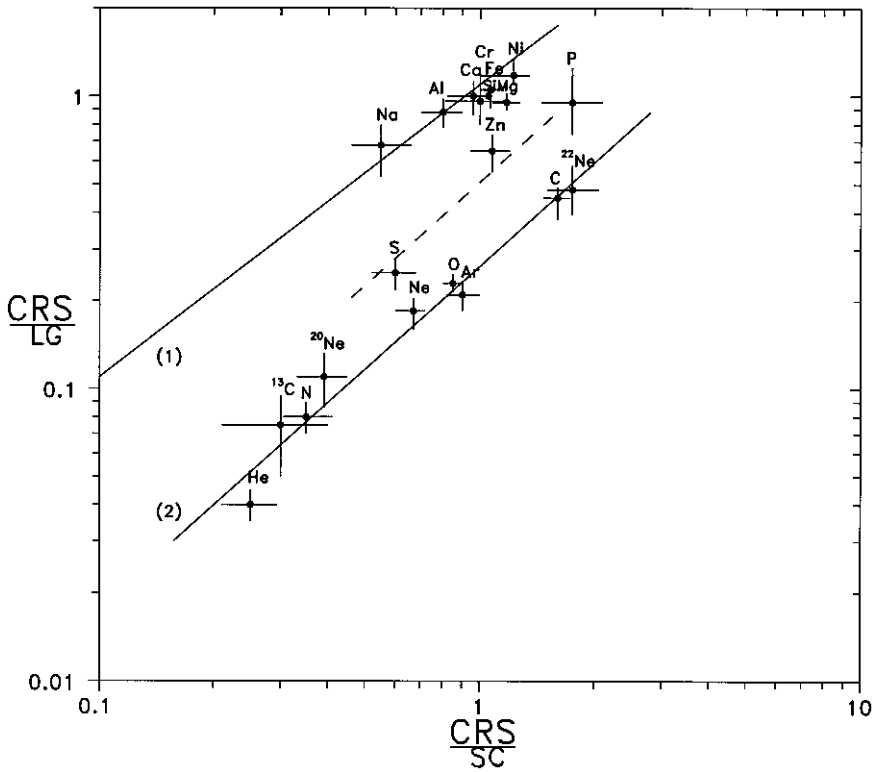

Figure 8. The CRS/LG ratio (vertical axis) vs SC/LG ratio (horizontal axis) for different classes of FIP elements.

5.2. ISOTOPIC COMPOSITION MEASUREMENTS

5.2.1. *Primary Nuclei*

Here again the recent *Voyager* and *Ulysses* data have dramatically changed our view on the isotopic compositional features of the CRS. As little as 8 years ago specific isotopic compositional differences between the CRS and solar system material were believed to be fairly widespread (e.g., Mewaldt, 1989). These compositional differences included the isotopes ^{12}C, ^{13}C, ^{14}N, ^{18}O, ^{22}Ne, ^{25}Mg, ^{26}Mg, ^{29}Si, ^{30}Si, ^{58}Fe, ^{58}Ni, and ^{60}Ni among the source nuclei. Improved cross section data relevant to the interstellar propagation as well as data of greatly improved statistical accuracy from *Voyager* (e.g., Lukasiak et al., 1997a) and *Ulysses* (Connell and Simpson, 1997) have reduced this number to three, ^{12}C or ^{13}C, ^{14}N and ^{22}Ne with the possible addition of ^{57}Fe. All of the other isotopes listed above appear to have essentially solar abundances within $\pm$10%. Table II (from Lukasiak et al., 1997a) gives a summary of the latest reported CRS/LG isotopic ratios.

This new data means that theories specifically developed to explain the earlier compositional differences must now be re-examined. But theories which involve

Table II
Cosmic-ray source/solar system[a] isotope ratios

Ratio	Voyager Measurements (Webber et al., 1997 + Lukasiak et al., 1997)	Other recent measurements	Prediction[d]
$^{13}C/^{12}C$	0.09 ± 0.36		0.6 W–R
$^{14}N/^{16}O$	0.41 ± 0.04		
$^{15}N/^{16}O$	2.62 ± 1.65		
$^{18}O/^{16}O$	1.04 ± 0.72		0.7 W–R
$^{22}Ne/^{20}Ne$	4.72 ± 0.43		3.5 W–R
$^{25}Mg/^{24}Mg$	1.06 ± 0.12		1.5 W–R
$^{26}Mg/^{24}Mg$	1.15 ± 0.11		1.5 W–R
$^{29}Si/^{28}Si$	0.80 ± 0.18		1.8 SM
$^{30}Si/^{28}Si$	1.03 ± 0.16		1.8 SM
$^{34}S/^{32}S$	1.07 ± 0.67	1.41 ± 0.66[b]	1.8 SM
$^{40}Ca/^{56}Fe$	1.16 ± 0.10		
$^{52}Cr/^{56}Fe$	1.51 ± 0.68		
$^{55}Mn/^{56}Fe$	1.35 ± 0.48		
$^{54}Fe/^{56}Fe$	0.93 ± 0.14	1.50 ± 0.10[c]	1.5 SM
$^{58}Fe/^{56}Fe$	1.48 ± 0.75	0.50 ± 0.35[c]	1.8 SM
$^{59}Co/^{56}Fe$	1.23 ± 0.40		
$^{58}Ni/^{56}Fe$	0.96 ± 0.15	0.95 ± 0.11[c]	
$^{60}Ni/^{56}Fe$	0.99 ± 0.24	1.23 ± 0.18[c]	
$^{62}Ni/^{56}Fe$	0.76 ± 0.40	0.90 ± 0.35[c]	

[a]From Cameron (1982);
[b]Thayer (1997);
[c]Connell and Simpson (1997);
[d]from Mewaldt (1989).
(W–R = Wolf–Rayet model, SM = supermetallicity model).

Wolf–Rayet (W–R) stars as source material for at least some fraction of the cosmic rays are still viable. These giant stars are known to produce copious amounts of ^{22}Ne through the process $^{14}N(\alpha,\gamma)\ ^{18}F(\beta^{+}\nu)\ ^{18}O(\alpha,\gamma)\ ^{22}Ne$, which uses up both ^{14}N and ^{4}He. This feature alone could explain the low relative abundances of both ^{4}He and ^{14}N in the CRS as well as the overabundance of ^{22}Ne. Just how much of this material is actually carried into the interstellar medium by the powerful W–R winds, to be eventually accelerated as galactic cosmic rays, remains uncertain however (see, e.g., Prantzos et al., 1986, 1990).

Using the isotopic abundance differences for ^{13}C and ^{22}Ne at the CRS source given in Table II and the abundance ratios for the C and Ne charges themselves listed in Table I we have placed the abundances of ^{13}C, ^{12}C, ^{22}Ne, and ^{20}Ne in the CRS individually in Figure 8 along with the other charge ratios. All of these

isotopes have a high FIP and lie along the separate high FIP line. The spread of ratios along this line could directly reflect CRS abundance differences with respect to the SC. In this case the isotopes ^{12}C and ^{22}Ne are overabundant by a factor 1.6–1.8 while ^{4}He, ^{13}C, ^{14}N, and ^{20}Ne are all underabundant by factors of between 0.25–0.40. The low ^{13}C/^{12}C abundance ratio observed in the CRS is thus a reflection of *both* a high ^{12}C abundance and a low ^{13}C abundance. Both ^{16}O (and ^{18}O) and Ar have similar abundances in both the CRS and the SC. This pattern of abundance differences is similar to that inferred for a W–R source contribution although the actual factors from recent calculations are somewhat different (e.g., Prantzos et al., 1986). For the intermediate FIP elements, the abundance of S in the CRS is seen to be lower than in the SC. For the low FIP elements, all of those shown in Figure 8 have similar abundances in both sources with the exception of Na.

In this picture the abundance differences between the CRS and LG are a combination of FIP differences which match those seen in the SC and actual source abundance differences. It is not necessary to introduce volatility to explain the differences. The model by Meyer et al. (1997) discussed in the previous section which does use volatility in place of FIP, as well as some W–R related compositional differences to explain the CRS – LG differences, is certainly a very interesting alternative, however. Differences in the two explanations may depend on measurements of $Z > 30$ nuclei abundances which are not known as accurately and are not likely to be improved upon in the near future.

5.2.2. *Decaying Source Nuclei*

Casse and Soutoul (1978) first noted that ^{57}Ni and ^{59}Ni, both radioactive and produced in the Fe peak nucleosynthesis in the last throes before a SN explosion, might be used to date the time of acceleration of cosmic rays. At low energies, before acceleration, these nuclei will decay by K-electron capture but after acceleration this decay will be much less likely since it is more difficult to retain a K-electron. In the presence of K-electrons, ^{57}Ni decays quickly to ^{57}Co which then decays with a half-life of 270 days to ^{57}Fe. In Figure 9 we show measurements of the isotopic composition of Co nuclei from the ISEE and *Voyager* spacecraft. Some ^{57}Co is observed but this is consistent with interstellar production, the original much larger amount of ^{57}Co having decayed to ^{57}Fe. The decay of ^{59}Ni is another matter, however. The interstellar production of ^{59}Co is expected to be only $\sim$30% of that of ^{57}Co so the excess amount of ^{59}Co observed in the cosmic-ray data indicates some, but perhaps not all, of the ^{59}Ni (half-life $= 7 \times 10^4$ yr) has decayed. Using the ^{59}Co data alone, Lukasiak et al. (1997b) have estimated that the delay between the production and acceleration of ^{59}Ni to high energies is $> 3 \times 10^4$ yr at the 2σ level. However, this question may also be answered by looking to see if any ^{59}Ni remains. Figure 10 shows the mass distribution of Ni events from the *Ulysses* spacecraft (Connell and Simpson, 1997). Here clear evidence for some ^{59}Ni is observed, however, of the 10 ^{59}Ni events seen, $\sim$5 are accounted for by interstellar production. If no ^{59}Ni has decayed at all, $\sim$35 events would be expected, so the

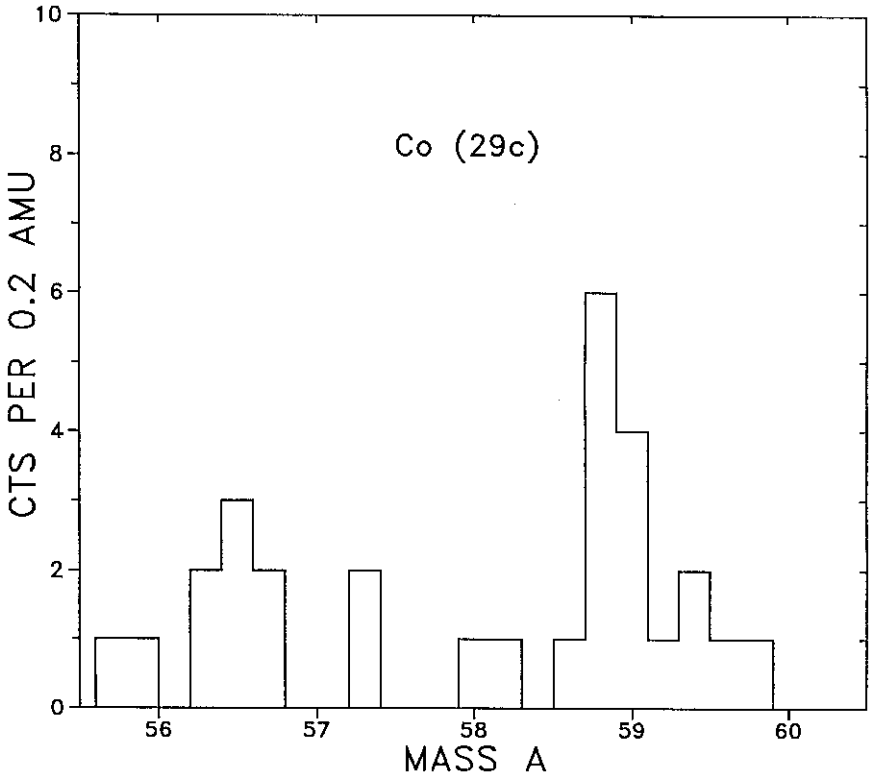

Figure 9. Isotopic abundance of cosmic-ray Co nuclei from the combined ISEE (Leske, 1993) and *Voyager* (Lukasiak et al., 1997b) measurements.

Ni data by itself suggests that indeed most of the ^{59}Ni has decayed. By combining both the Co and Ni data one reaches the conclusion that the initial acceleration to high energies occurs at least 7×10^4 yr after the nucleosynthesis. In such a case the accelerated cosmic rays are unlikely to be directly accelerated ejecta from the SN themselves but could be interstellar matter or stellar coronal material from local stellar winds.

5.2.3. *Decaying Secondary Nuclei*

Here we are not so much interested in the radioactive decay secondary nuclei with fixed half-lives such as ^{10}Be and ^{26}Al which provide valuable information on the propagation time of cosmic rays, but rather on certain secondary K-electron capture nuclei. These K capture nuclei will only decay if they can pick-up a K shell electron during propagation. This attachment process is strongly energy dependent – and is essentially zero at energies ≥ 1 GeV nucl^{-1}. At low energies the increasing likelihood of attachment means that the effective lifetime for K-capture decay is strongly energy dependent. A list of K-capture isotopes (all produced as secondaries during interstellar propagation after an assumed initial acceleration)

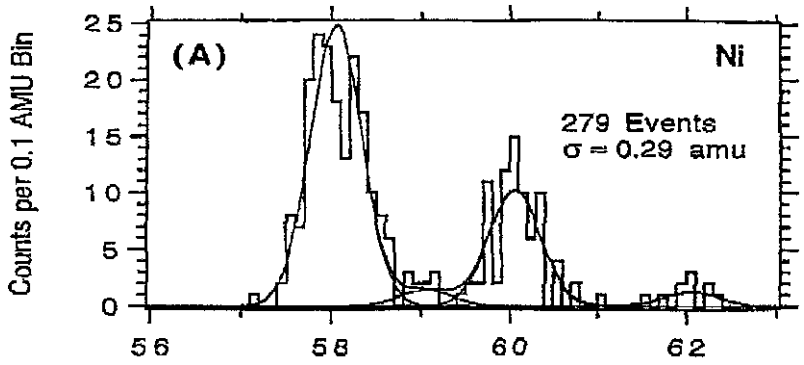

Figure 10. Isotopic abundance of cosmic-ray Ni nuclei from the *Ulysses* measurement (Connell and Simpson, 1997).

and their effective lifetimes and surviving fractions in the interstellar medium as a function of energy is given in Table III (see also discussion by Letaw et al., 1984). The amount of this decay that is observed can be used to estimate the interstellar energy at which the decay occurs. Given accurate predictions of the production of these nuclei based on propagation models and cross sections for their production, it should be possible to determine whether this production energy is the same as the energy observed now – in essence to measure the effects of re-acceleration. This suggestion was first made by Raisbeck et al. (1975). The first attempts to utilize this effect to estimate possible re-acceleration effects suffered from poorly known cross sections and cosmic-ray data that was only slightly better. Now, however, cross section measurements of the required precision exist and *Voyager* data on the isotopes of the Fe group nuclei, specifically the elements Ti, V, and Cr, have shown convincingly for the first time that this decay is occurring and have, in fact, used the amount of decay to set rough limits on possible interstellar re-acceleration (Soutoul et al., 1997).

This analysis uses measurements of the isotopic composition of V nuclei with confirming evidence from Ti and Cr. The distribution of V isotopes observed by the *Voyager* and ISEE spacecraft is shown in Figure 11 along with the predicted distribution if no K-capture decay occurs. The abundance of ^{49}V is clearly less than expected, indicating decay. (The ^{49}Ti abundance is found to be correspondingly higher.) The ^{51}V abundance is much higher than expected indicating that ^{51}Cr has decayed. (The ^{51}Cr abundance is indeed correspondingly lower.) Overall this data suggests that between 25–30% of these two K-capture nuclei have decayed. This is significantly larger than the 10% expected at an interstellar energy which is equal to the energy observed at the Earth $+\phi$, the energy lost in interplanetary space in the standard solar modulation picture (Goldstein et al., 1970). In order to observe a decay of $\sim$25–30%, the particles must have originated at an energy $\sim$100 MeV nucl^{-1} less than their presently implied interstellar energy of 500 MeV nucl^{-1}. This suggests a possible energy gain $\sim$20%, but because of

Table III
K-capture isotopes

	$\tau(10^6\text{yr})$ 350–500–650 MeV nucl^{-1}	f 500 MeV nucl^{-1}	cts		cts
^{37}Ar	40–75–90	0.96	200	$\rightarrow^{37}$Cl	35
^{44}Ti	18–30–48	0.93	20	$\rightarrow^{44}$Ca	330
^{49}V	12–22–36	0.90	250	$\rightarrow^{49}$Ti	200
^{51}Cr	9–18–30	0.88	400	$\rightarrow^{51}$V	180
^{54}Mn	7.5–13–24	0.85	100	$\rightarrow^{54}$Cr	80
^{55}Fe	6–10–20	0.82	300	$\rightarrow^{55}$Mn	400
^{57}Co	4.5–7.5–16	0.78	30	$\rightarrow^{57}$Fe	450

τ = effective lifetime; f = surviving fraction; cts = number of events seen by both *Voyager* and *Ulysses*.

various uncertainties, including the effect of solar modulation, this value is more in the nature of an upper limit. This approach holds promise for finally providing some insight on this important aspect of the cosmic-ray acceleration process in our galaxy, however.

5.3. Measurements of the Energy Spectra of Nuclei

Considerable improvements of our understanding of the energy spectra of cosmic-ray nuclei at energies $\geq$ 100 GeV nucl^{-1} have occurred in recent years mainly as a result of the Spacelab and Sokol experiments and also from long duration balloon payloads. The spectra of the primary nuclei, H, He, and Fe are the best known but inconsistencies remain in the measurements of the O spectrum. The spectra of secondary nuclei such as B and Fe sec have also been extended to higher energies. In one study using both low energy measurements from the *Voyager* spacecraft and several new high energy measurements, Webber and McDonald (1994) have shown, using the He/O ratio variations with energy, that the He and O spectra appear to be identical within $\pm$0.03 in the spectral index over four orders of magnitude in energy from $\sim$100 MeV nucl^{-1} to over 10^{12} eV nucl^{-1}. This is less than the spectral variations between these charge components that is expected from nonlinear shock acceleration theories according to the calculations of Ellison (1993), for example.

The situation is not so straight forward when one simply compares the measured high energy spectral indices of the various charge components, however. The worlds most recently available data on the energy spectra of H, He, O, and Fe nuclei are summarized in Figure 12 (see also Swordy, 1994) The intensities and the average spectral indices between 20 and 2000 GeV nucl^{-1} for these components are given in Table IV along with comments on the intensities above 2000 GeV nucl^{-1}. For protons a spectral index $= -2.76 \pm 0.04$ is seen to fit essentially all of the data

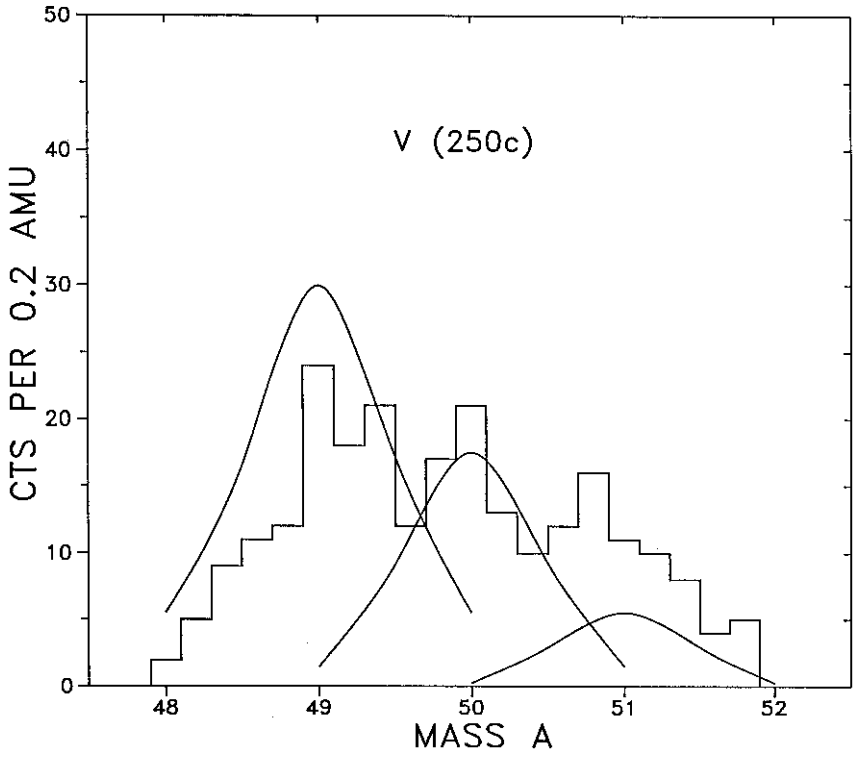

Figure 11. Isotopic abundance of cosmic-ray V nuclei from the combined ISEE (Leske, 1993) and *Voyager* (Lukasiak et al., 1997) measurements. Differences between measurements and predictions (shown as a solid line) are attributed to the decay of the K capture nuclei ^{51}Cr (which increases ^{51}V) and ^{49}V (which is lower than expected).

from ∼20 GeV up to at least 2×10^4 GeV. For He nuclei a single spectral index $= -2.66$ also fits all of the data – with perhaps somewhat larger uncertainties. For Fe nuclei a single spectral index $= -2.61 \pm 0.07$ fits all of the current data between 20–2000 GeV nucl^{-1}. This suggests that the spectra of He and Fe nuclei may be slightly flatter than that of H nuclei (see also the papers by Biermann et al., 1994; and Wiebel-Sooth et al., 1995, which reach a similar conclusion regarding the spectral differences of various charge species using somewhat earlier data). Problems exist in the interpretation of the O nuclei spectra, however. Considering only the data up to 2000 GeV nucl^{-1}, this spectrum can be fit with an index $= -2.66 \pm 0.07$, about the same as for He nuclei. The higher energy spectral points for O nuclei, from Asakamori et al. (1993) are a factor ∼1.5× higher than the extrapolation of the lower energy points. If these higher energy points are assumed to be correct then the average spectral index for O nuclei up to ∼2 x 10^4 GeV nucl^{-1} is $= -2.62 \pm 0.05$, about the same as that for Fe nuclei.

In order to claim that the spectral index of cosmic-ray nuclei decreases in a systematic charge dependent way from -2.76 for H to perhaps -2.61 for Fe

Table IV
High-energy spectra and intensities (from Figure 14)

Spectral index	Intensity ($\times E^{2.5}$) $20 \leq E \leq 2000$ GeV nucl^{-1}	GeV nucl^{-1} at 20	Data above 2000	2000 GeV nucl^{-1}
Protons	-2.76 ± 0.04	9.2×10^3	3.1×10^3	OK
Helium	-2.66 ± 0.05	390	200	OK
Oxygen	-2.66 ± 0.07	13.5	(6.5)	Factor 1.5 high ?
Iron	-2.61 ± 0.07	1.8	1.1	none

Intensities in particles m^{-2}sr^{-1}s^{-1}(GeV nucl^{-1})$^{-1}$ $\times$ (GeV nucl^{-1}).

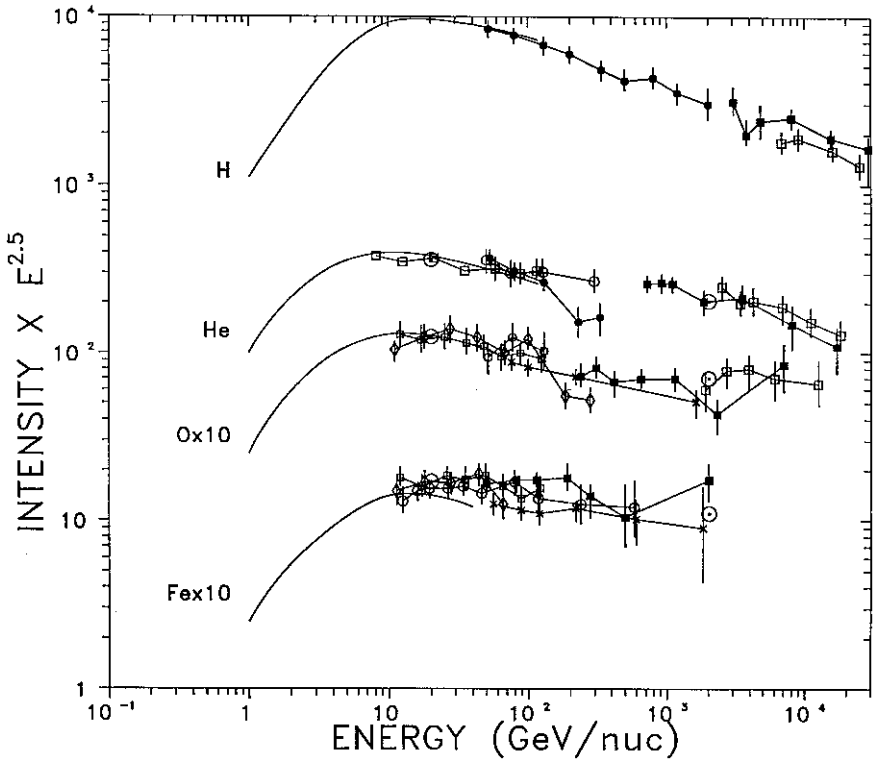

Figure 12. Summary of intensity measurements of the spectra of H, He, O, and Fe nuclei at high energies. The data (all $\times E^{2.5}$) are indicated as follows; solid lines, HEAO data for O and Fe (Engelmann et al., 1990), magnet data for H and He (Webber et al., 1987). Solid circles: Ryan et al. (1972). Solid squares: Ivanenko et al. (1993). Open squares: Asakamori et al. (1993). Open diamonds: Simon et al. (1980). Crosses: Müller et al. (1991). Open circles: Ichimura et al. (1993). Open squares (lower E) various gas Cerenkov data, Large circles with dot = normalization at 20 and 2000 GeV nucl^{-1}.

nuclei will require that the intensity differences for O nuclei above and below $\sim$2000 GeV nucl^{-1} be resolved. Even so there seems to be strong evidence that the high energy spectral indices of at least the most prominent $Z \geq 2$ nuclei are indeed somewhat flatter than that of H by $\sim$0.10 in the index. This difference may be explained by a model in which protons and heavier nuclei come from different sources (Biermann et al., 1994) or may reflect systematic variations of the spectral indices of individual charges as predicted by theories of shock acceleration in SNR (e.g., the predictions of the theory of Ellison et al, 1997, discussed earlier and shown in Figure 6).

5.3.1. *Secondary to Primary Ratios*

Another important feature of the high-energy measurements is the ratio of secondary to primary species as a function of energy. The energy dependence of this ratio is thought to map the escape length of cosmic rays from the galaxy and so to provide information on the energy dependence of the diffusion coefficient at high energies (see, however, the discussion by Biermann, 1996, which points out a situation where the two might not be equivalent). Both the B/C and Fe sec/Fe ratios can be used for this study, but recent data from the HEAO spacecraft (Binns et al., 1988) and balloon borne emulsion chambers (Ichimura et al., 1993) extend this ratio to several hundred GeV nucl^{-1} for Fe sec. This ratio is shown in Figure 13, along with various predictions. First of all it should be noted that their appears to be a kink in the observed ratio at $\sim$10 GeV nucl^{-1}, the ratio having a steeper energy dependence below 10 GeV nucl^{-1} and a flatter energy dependence above this energy (see, e.g., Webber, 1993). This may be due to the fact that the energy dependence of the fragmentation cross sections into Fe sec begins to be important below 10 GeV nucl^{-1}. If one carefully fits the observed energy dependence both above and below 10 GeV nucl^{-1}, using the simple Leaky box propagation model, but including energy dependent cross sections extending up to 10 GeV nucl^{-1} (which were not included above 2 GeV nucl^{-1} in earlier calculations), then the dependence above 10 GeV nucl^{-1} is found to be $\sim R^{-0.50\pm0.05}$ as shown in Figure 13. This escape length dependence of -0.50 at the high energies is certainly inconsistent with an escape length controlled by a Kolomogorov type of turbulence which is $\sim R^{-0.33}$. Models in which re-acceleration is prominent predict a flattening of the secondary to primary ratios above $\sim$10 GeV. If this flattening is to the Kolomogorov index of -0.33 as in the case of the calculations by Heinbach and Simon (1995) and Seo and Ptuskin (1994) it is obvious from the curves in Figure 13, taken from their respective papers, that these models actually give a very poor fit to the data for the Fe sec/Fe ratio. More work is needed in the theoretical area to fully understand this new behavior of the escape length dependence brought about by energy dependent cross sections.

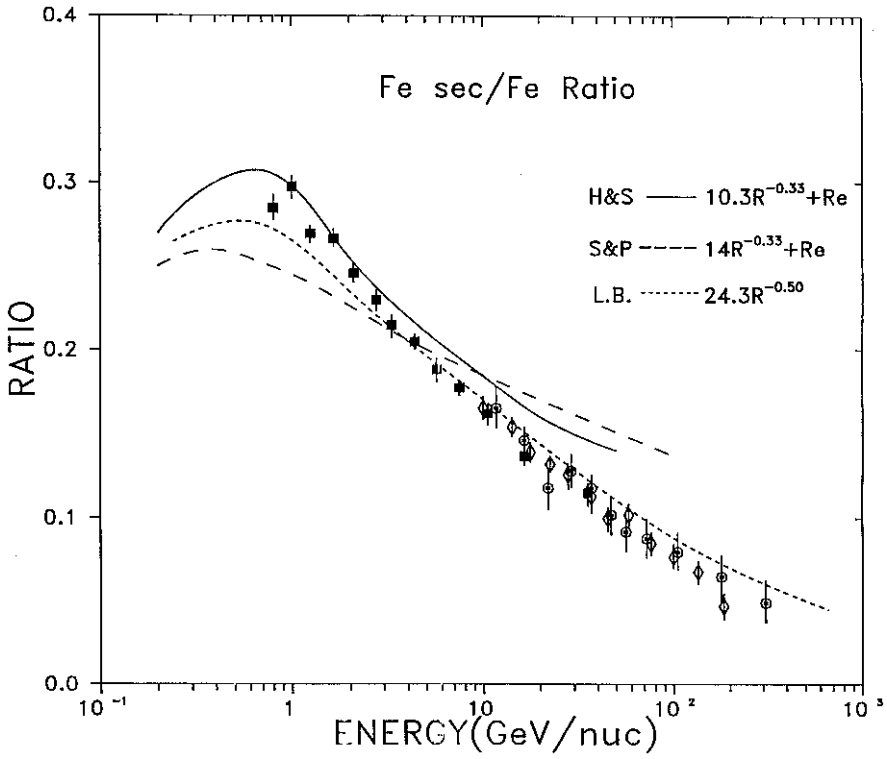

Figure 13. Measurements of the $Z = 21 - 23$/Fe ratio as a function of energy along with predictions. The data are indicated as follows; solid squares, HEAO data (Engelmann et al., 1990), open diamonds HEAO data (Binns et al., 1988), circles with crosses, balloon data, (Ichimura et al., 1993). The predictions of two reacceleration models (Seo and Ptuskin, 1994; Heinbach and Simon, 1995) are shown along with the predictions of a simple Leaky box model with an escape length $\sim P^{-0.5}$ at all energies but including energy dependent cross sections up to 10 GeV nucl^{-1}.

6. Summary and Outlook

There have been substantial new advances in several experimental areas relating to the sources and to the origin and acceleration of cosmic rays in galaxies. These advances can be grouped into three broad areas: (1) The energetics of cosmic rays in our galaxy, (2) Astrophysical observations in both radio astronomy and γ-ray astronomy which provide information on the sites of cosmic-ray acceleration and how these particles are re-distributed throughout our galaxy and other nearby galaxies, and (3) Cosmic-ray observations themselves which give a clearer picture of the elemental and isotopic composition and the energy spectrum of these particles which in turn relate directly to the sites of acceleration and the mechanism of acceleration.

In conjunction with the energetics, data from spacecraft in the outer heliosphere have shown that the local energy density of all cosmic rays, including electrons is

$\sim$2eV cm^{-3}, or about twice the commonly assumed value. Propagation models also indicate that these particles have traversed more matter than previously thought; $\sim$10 g cm^{-2} at $\sim$1 GeV nucl^{-1} in contrast to earlier estimates of $\sim$5 g cm^{-2}. Thus altogether more energy is involved for galactic cosmic rays, both from the point of view of the energy requirements of the sources of cosmic rays and the energy dissipated in the interstellar space by ionization and other loss mechanisms. This ionization loss may make a significantly larger contribution to the interstellar ionization state in our galaxy than has been previously assumed, including a significant contribution to the diffuse ionized layer that extends beyond the matter disk to perhaps $\pm$1 Kpc in the Z direction.

The details of the interstellar electron spectrum can now be followed down to energies of a few MeV from γ-ray measurements by COMPTEL. This evidence suggests that the electron spectrum continues with an index ~ -2.0, flattening somewhat at lower energies due to ionization loss, down to a few MeV. This indicates that, energetically, the electron contribution in our galaxy is 20–30% of that of cosmic-ray nuclei – much larger than the 2–3% implied by higher energy measurements.

Both radio astronomy and γ-ray astronomy have contributed to a better understanding of the sources of cosmic rays in our galaxy and in nearby galaxies. Radio astronomical observations, which have much higher angular resolution and sensitivity than γ-ray observations, are sensitive only to electrons, however. They show that the strongest sources of these electrons, accelerated with spectral indices $\sim$2 + ϵ, occur in association with SNR both in our galaxy and M-33. Details of the electron acceleration within these SNR can be observed in several cases in our own galaxy. These measurements show a complex pattern of acceleration associated with strong large scale shock structures throughout the remnants. γ-ray observations above 100 MeV show several strong sources associated with SNR in our galaxy and are suggestive of accelerated cosmic-ray nuclei interactions with local matter in these sources. Thus a strong case can be made for the acceleration of both primary electrons and nuclei in these sources from the new observations.

Detailed studies of the total radio power emitted by nearby galaxies such as M-33, and the power emitted from SNR in the same galaxy, can be used to infer that the SNR are indeed the sources of the globally distributed electrons in that galaxy. Measurements of the radio profiles along the disks, and perpendicular to the disks (e.g., the extent of galactic halos) of $\sim$10 nearby galaxies show distributions of energetic electrons that are consistent with the distribution of electrons inferred for our own galaxy which has an e-folding Z distance $\sim$1.0 Kpc.

New cosmic-ray composition observations from the *Voyager* and *Ulysses* spacecraft have now provided information on the CRS abundance of $\sim$25 individual isotopes in the charge range $Z = 6 - 28$. Only 4 of these, ^{4}He, ^{22}Ne, ^{14}N, and the ^{13}C/^{12}C ratio have a clearly non-solar abundance. These specific abundance differences point to a Wolf–Rayet contribution to the source composition. The determination of the charge composition at the cosmic-ray source has also stead-

ily improved – as a result of better measurements from the *Voyager* and *Ulysses* spacecraft and more refined propagation models utilizing new cross section measurements. The previously observed deficiency of high FIP elements relative to LG composition continues to be well established. The similarity of this effect to what is seen when solar photospheric abundances are compared with solar coronal abundances has given support to a picture in which the acceleration process at the CRS operates on coronal type interstellar material. However several elements which have a high volatility such as Na, P, Ge, and possibly Pt also appear to the underabundant in the CRS. This has led to the suggestion that both volatility and refractivity play a role in the injection process as well.

The abundance of various types of radioactive decay isotopes continues to play an important role in understanding the acceleration and possible re-acceleration of the cosmic-ray material. The ^{59}Ni produced at the time of Fe nucleosynthesis in SN appears to have mostly decayed to ^{59}Co, but a small fraction may still remain at the time of the cosmic-ray acceleration. Since the half-life of this isotope is $\sim 7 \times 10^4$ yr, this would place the characteristic time of the cosmic-ray acceleration at least 7×10^4 yr after nucleosynthesis, a time delay that is only compatible with the acceleration of ambient interstellar or hot coronal material.

Clear evidence for the decay of the K capture isotopes ^{51}Cr and ^{49}V also has been observed. This decay would be expected at low energies during the normal propagation of these nuclei as the result of electron attachment. This attachment is strongly energy dependent and the observed decay $\sim$25% of these isotopes is more than the 10% expected at their current interstellar energy. This suggests a possible energy gain of up to $\sim$100 MeV nucl^{-1} of their current interstellar energy $\sim$500 MeV nucl^{-1}. This may be the first hard evidence that interstellar re-acceleration does occur but at a level less than that necessary to greatly modify the spectra and charge ratios of the secondary/primary cosmic rays.

Much new data is also available on the energy spectra of the various primary charge components ranging from H to Fe. This data is mostly at higher energies above $\sim$100 GeV nucl^{-1} although some data is also available at interstellar energies $\sim$300–400 MeV nucl^{-1}. A comparison of the measured He/O ratio with predictions of propagation models from these low energies up to a few TeV nucl^{-1} shows no changes that cannot be accounted for by propagational effects, thus indicating similar spectra to within ± 0.03 in the exponents. A comparison of the relative spectra of individual nuclei cannot be made to such a high level of precision, however. Generally the measurements of the spectral index of all charge components above $\sim$100 GeV nucl^{-1} approach a value in the range -2.75 (for H) to -2.65 (for $Z \geq 2$ nuclei), but specific differences in the spectral index for different heavier charges are at the limit of detection, given the current uncertainties of ± 0.05 in the spectral index.

The outlook for improved data in all areas is extremely bright. By the year 2000 the *Voyager* spacecraft are expected to have reached the solar wind termination shock. At this time we will have a much better understanding of the acceleration of

the anomalous component, including the fraction of solar wind energy actually converted, the actual spectrum at the shock and perhaps what fraction of this component actually escapes the heliosphere. The first observations outside the shock will also give information on the lowest energy part of the spectra for all of the galactic cosmic-ray components which have hitherto been unobservable from within the heliosphere. This may include possible localized low energy ($\sim$10 MeV nucl^{-1}) components such as those responsible for providing γ-ray lines from the vicinity of the Orion complex (Bloemen et al., 1994).

The study of cosmic-ray electrons in our galaxy and other galaxies will benefit from radio-astronomical measurements with improved angular resolution over a broad range of frequencies from telescopes such as the VLA or the Australian Telescope. This will lead to an improved understanding of electron acceleration in SNR in our galaxy and other nearby galaxies as well as the actual distribution of these electrons, particularly in the halos of other galaxies. This data can be combined with the many new surveys of the Hα and FIR distributions in these galaxies which can help pinpoint the sources of the energetic electrons. And finally continued studies of SNR by the EGRET instrument on GRO may provide a better picture of the acceleration of cosmic-ray nuclei in these objects. EGRET has the potential of setting further limits on the γ-ray emission from members of the local group of galaxies thus furthering our understanding of cosmic-ray nuclei acceleration in these objects, many of which have already been studied using radio frequencies for information related to electron acceleration.

For cosmic-ray observations themselves we have the prospect of continued data from *Voyager* and particularly from *Ulysses* – thus adding to the statistical accuracy of the data and providing improved estimates of the cosmic-ray source charge and isotopic composition. These measurements over the period of low solar modulation around the current sunspot minimum period which extends from 1995, 1996, and probably through 1997, will be important for studying the decay of K-capture isotopes. In this connection the isotope data from the large area telescope on the WIND spacecraft launched in Nov. 1994 may also make a significant advance. However, the major advance in all the areas of charge and isotope studies should occur in 1997 with the launch of the ACE spacecraft. This spacecraft will provide data with greater than 10$\times$ the statistical accuracy of all the previous measurements combined and should provide more definitive answers to many of the cosmic-ray observations discussed in this review. At high energies continued observations are being made, including studies of the hydrogen, helium and heavier nuclei spectra up to and above 1 Tev nucl^{-1} using emulsions, magnets, and calorimeters on balloons. These measurements are important for resolving discrepancies in the measured spectral indices for these components.

References

Anderson, M. C. and Rudnick, L.: 1996, *Astrophys. J.* **456**, 234.
Asakamori, K. et al.: 1993, *Proc 23rd Int. Cosmic Ray Conf., Calgary* **2**, 21.
Axford, W. I.: 1981, *Proc 17th Int. Cosmic Ray Conf., Paris* **12**, 155.
Beck, R.: 1994, *Publ. Astron. Soc. Pacific* **18**, 43.
Beck, R. and Golla, G.: 1988, *Astron. Astrophys.* **191**, L9.
Berkhiujsen, E.: 1996, *Astron. Astrophys.* **166**, 257.
Bicay, M. D. and Helou, G.: 1990, *Astrophys. J.* **362**, 59.
Biermann, P. L.: 1996, '*Mission 96' Workshop*, *Acta Physica Polonica B.* **27**, 3399.
Biermann, P. L., Gaisser, T. K., and Stanev, T.: 1994, *Phys. Rev.* **D51**, 3450.
Binns, W. R. et al.: 1988, *Astrophys. J.* **324**, 1106.
Blandford, R. D. and Ostriker, J. P.: 1978, *Astrophys. J.* **221**, L229.
Blandford, R. D. and Ostriker, J. P.: 1980, *Astrophys. J.* **237**, 793.
Blandford, R. D. and Eichler, D.: 1987, *Phys. Reports* **154**, 1.
Bloemen, J. B., Dogiel, V. A., Dorman, V. L., and Ptuskin, V. S.: 1993, *Astron. Astrophys.* **267**, 372.
Bloemen, J. B. et al.: 1994, *Astron. Astrophys.* **281**, L5.
Cameron, A. W.: 1982, in C. A. Barnes, D. D. Clayton, and D. N. Schramm (eds.), *Essays in Nuclear Astrophysics*, Cambridge University Press, New York, p. 23.
Casse, M. and Soutoul, A.: 1978, *Astrophys. J.* **200**, L75.
Cesarsky, C. J.: 1987, *Proc. 20th Int. Cosmic Ray Conf., Moscow* **8**, 87.
Chevaliar, R. A., Robertson, J. W., and Scott, J. S.: 1976, *Astrophys. J.* **207**, 450.
Connell, J. J. and Simpson, J. A.: 1997, *Astrophys. J.* **475**, L61.
Dahlem, M., Lisenfeld, U., and Golla, G.: 1995, *Astrophys. J.* **444**, 119.
Decker, R. B.: 1988, *Space Sci. Rev.* **48**, 195.
de Jong, T., Klein, U., Wielebinski, R., and Wunderlich, E.: 1985, *Astron. Astrophys.* **147**, L6.
Devereaux, N. A. and Eales, S. A.: 1989, *Astrophys. J.* **340**, 708.
Dickey, J. M. and Salpeter, E. E.: 1984, *Astrophys. J.* **284**, 461.
Drury, L.: 1983, *Rep. Prog. Phys.* **46**, 973.
Duvernois, M. A. and Thayer, M. R.: 1996, *Astrophys. J.* **465**, 982.
Duric, N.: 1988, *Space Sci. Rev.* **48**, 73.
Duric, N.: 1994, *Publ. Astron. Soc. Pacific* **18**, 17.
Duric, N. et al.: 1995, *Astrophys. J.* **445**, 173.
Ellison, D. C., 1993, *Proc. 23rd Int. Cosmic Ray Conf., Calgary* **2**, 219.
Ellison, D. C. and Reynolds, S. P.: 1991, *Astrophys. J.* **382**, 242.
Ellison, D. C., Drury, L., and Meyer, J. P.: 1997, *Astrophys. J.* (in press).
Engelmann, J. J. et al.: 1990, *Astron. Astrophys.* **233**, 96.
Esposito, J. A., Hunter, S.D., Kanbach, G., and Sreekumar, P.: 1996, *Astrophys. J.* **461**, 820.
Fermi, E.: 1949, *Phys. Rev.* **75**, 1169.
Fisk, L. A., Kozlovsky, B., and Ramaty, R.: 1974, *Astrophys. J.* **190**, L35.
Garrard, T. L. and Stone, E. C.: 1993, *Proc. 23rd Int. Cosmic Ray Conf., Calgary* **3**, 384.
Ginzburg, V. L. and Syrovatskii, S. I.: 1964, *The Origin of Cosmic Rays*, Pergamon, Oxford.
Goldstein, M. L., Fisk, L. A., and Ramaty, R.: 1970, *Phys. Rev. Letters* **25**, 832.
Green, D. A., 1984, *Monthly Notices Roy. Astron. Soc.* **209**, 449.
Grevesse, N. and Anders, E.: 1989, in C. J. Waddington (ed.), *Cosmic Abundances of Matter*, AIP Conf. Proc. No. 183 N.Y. AIP Press, p. 1.
Heikkila, B. and Webber, W. R.: 1994, *Proc. Workshop on High Spatial Res. For Infrared Data*, JPL Pub. 94–5, p. 95.
Heinbach, U. and Simon, M.: 1995, *Astrophys. J.* **441**, 209.
Hovestadt, D., Vollmer, O., Gloeckler, G., and Fan, C. Y.: 1973, *Phys. Rev. Letters* **31**, 650.
Hunter, S. D. et al.: 1997, *Astrophys. J.* **481**, 205.
Ichimura, M. et al.: 1993, *Phys. Rev.* **D48**, 1949.
Ip, W. H. and Axford, W.I.: 1985, *Astron. Astrophys.* **149**, 7.
Ivanenko, I. P. et al.: 1993, *Proc. 23rd Int. Cosmic Ray Conf., Calgary* **2**, 17.
Jokipii, J. R.: 1986, *J. Geophys. Res.* **91**, 2929.

Jokipii, J. R.: 1990, in S. Gzedzielski and D. E. Page (eds.), *Proc. of COSPAR-Colloquium – 'Physics of the Outer Heliosphere' Warsaw*, Pergamon, Oxford, p. 169.
Jones, F. C. and Ellison, D. C.: 1991, *Space Sci. Rev.* **58**, 259.
Leske, R. A.: 1993, *Astrophys. J.* **405**, 567.
Letaw, J. R., Silberberg, R., and Tsao, C.H.: 1984, *Astrophys. J. Suppl.* **56**, 369.
Letaw, J. R., Silberberg, R., and Tsao, C. H.: 1993, *Astrophys. J.* **414**, 601.
Lukasiak, A., Ferrando, P., McDonald, F. B., and Webber, W. R.: 1994, *Astrophys. J.* **423**, 426.
Lukasiak, A., McDonald, F. B., and Webber, W. R.: 1997a, *Astrophys. J.* (in press).
Lukasiak, A., McDonald, F. B., Webber, W. R., and Ferrando, P.: 1997b, *Adv. Space Res.* **19**, 747.
McDonald, F. B., Teegarden, B. J., Trainor, J. H., and Webber, W. R.: 1974, *Astrophys. J.* **51**, L217.
Mewaldt, R. A.: 1989, in C. J. Waddington (ed.), *Cosmic Abundances of Matter*, AIP Conf. Proc No. 183, AIP Press, New York, p. 124.
Mori, M.: 1997, *Astrophys. J.* **478**, 225.
Müller, D., Swordy, S. P., Meyer, P., L'Heureux, J., and Grunfeld, J. M.: 1991, *Astrophys. J.* **374**, 356.
Pesses, M. E., Jokipii, J. R., and Eichler, D.: 1981, *Astrophys. J.* **246**, L85.
Prantzos, N., Doom, C., Arnould, M., and deLoore, C.: 1986, *Astrophys. J.* **304**, 695.
Prantzos, N., Meyer, J. P., and Arnould, M.: 1990, *Proc. 22nd Int. Cosmic Ray Conf., Adelaide* **4**, 51.
Raisbeck, G. M., Comstock, G., Perron, C., and Yiou, F.: 1975, *Proc 14th Int. Cosmic Ray Conf., Münich* **2**, 560.
Reames, D. V.: 1995, *Adv. Space Res.* **15**, 41.
Reynolds, S. P. and Ellison, D. C.: 1992, *Astrophys. J.* **399**, L75.
Ryan, M. J., Ormes, J. F., and Balasubrahmanyan, V. K.: 1972, *Phys. Rev. Letters* **28**, 985.
Seo, E. S. and Ptuskin, V. S.: 1994, *Astrophys. J.* **431**, 705.
Simon, M. et al.: 1980, *Astrophys. J.* **239**, 712.
Simon, M., Heinrich, W., and Mathis, K. D.: 1986, *Astrophys. J.* **300**, 32.
Soutoul, A., Lukasiak, A., McDonald, F. B., and Webber, W. R.: 1997 *Astrophys. J.* (submitted).
Sreekumar, P. et al.: 1992, *Astrophys. J.* **400**, L67.
Stone, E. C., Cummings, A. C., and Webber, W. R.: 1996, *J. Geophys. Res.* **101**, 11017.
Strong, A. W. and Youssefi, G.: 1997, *Astron. Astrophys.* (in press).
Strong, A. W. and Mattox, J. R.: 1996, *Astron. Astrophys.* **308**, L21.
Swordy, S. P.: 1994, *Proc. 23rd Int. Cosmic Ray Conf.* **8**, 243.
Thayer, M. R.: 1997, *Astrophys. J.* **482**, 792.
Volk, H. J.: 1984, in J. Andouze (ed.), *High Energy Astrophysics*, Edition Frontière, p. 281.
Webber, W. R.: 1975, *Proc. 14th Int. Cosmic Ray Conf., Münich* **5**, 1597.
Webber, W. R.: 1987, *Astron. Astrophys.* **179**, 277.
Webber, W. R.: 1993, *Astrophys. J.* **402**, 188.
Webber, W. R.: 1994, *Publ. Astron. Soc. Pacific* **18**, 37.
Webber, W. R. and McDonald, F. B.: 1994, *Astrophys. J.* **435**, 464.
Webber, W. R., Simpson, G. A., and Cane, H. V.: 1980, *Astrophys. J.* **236**, 448.
Webber, W. R., Golden, R. L., and Stephens, S. A.: 1987, *Proc. 20th Int. Cosmic Ray Conf., Moscow* **1**, 325.
Webber, W. R., Lee, M. A., and Gupta, M.: 1992, *Astrophys. J.* **390**, 96.
Webber, W. R., Ferrando, P., Lukasiak, A., and McDonald, F. B.: 1992, *Astrophys. J.* **392**, L91.
Webber, W. R., Heikkila, B., and Templeton, M. R.: 1994, *Bull. 185th AAS Meeting*.
Webber, W. R., Lukasiak, A., and McDonald, F. B.: 1997, *Astrophys. J.* **476**, 766.
Wiebel-Sooth, B., Biermann, P. L., and Meyer, H.: 1995, *Proc. 24th Int. Cosmic Ray Conf., Rome* **2**, 656.
Zweibel, E. G. and Heiles, C.: 1997, Nature, **385**, 131.